Metal-Insulator Transition and Antiferromagnetism in a One-Dimensional Organic Solid*

A. J. Epstein, † S. Etemad, A. F. Garito, and A. J. Heeger
Department of Physics and Laboratory for Research on the Structure of Matter, University of Pennsylvania, Philadelphia, Pennsylvania 19104
(Received 16 April 1971; revised manuscript received 5 August 1971)

An experimental study of the organic charge-transfer salt *N*-methyl-phenazinium tetracyanoquinodimethan (NMP-TCNQ) is presented. Magnetic-susceptibility, specific-heat, spin-resonance, and conductivity measurements indicate a metallic state above 200 °K with a continuous transition to a small-band-gap magnetic Mott insulator below 200 °K. The ground-state and low-lying excitations indicate that this system can be quantitatively described in terms of the one-dimensional Hubbard model with a transfer integral of 2.1×10^{-2} eV and an effective Coulomb interaction of 0.17 eV. These values are discussed in terms of the fundamental molecular physics of the $TCNQ^-$ anion in the NMP-TCNQ crystal. It is concluded that in addition to the Heitler-London correlation which reduces the interaction between two excess electrons on a TCNQ molecule, the NMP cation polarizability plays a significant role in reducing the effective interaction. The transition to the metallic state is attributed to electron-hole correlations which become important when the number of excitations is large. These correlations persist into the metallic state where the electronic system behaves as a quasi-free-electron Fermi liquid as indicated by the unenhanced Pauli susceptibility and simple transport properties. The low-temperature one-dimensional antiferromagnetic state is studied using spin-resonance and specific-heat techniques. The linear temperature dependence of the specific heat predicted for the one-dimensional antiferromagnet has been observed. Electron-spin-resonance linewidth studies indicate motionally narrowed dipolar widths with the correlation time determined by the Fermi velocity in the metallic state and by exchange in the insulating state. The large fluctuations expected for a one-dimensional "phase transition" show up as a maximum in the correlation time, which however never exceeds 10^{-13} sec. The spin-lattice relaxation of the conduction electrons via phonons and molecular vibrations in the metallic state has been observed. The results are consistent with Elliot's theory in which $T_1^{-1}\sim(\Delta g/g)^2\tau_R^{-1}$, where τ_R is the scattering time as determined from the resistivity.

I. INTRODUCTION

The development of the one-electron band theory in the 1930's was clearly the fundamental step toward our present understanding of the solid state. The success of this theory in explaining many of the properties of solids is well known. However, in 1949 Mott[1] first raised the very interesting question of how one visualizes the transition from a collection of isolated atoms with localized bound electrons to a solid where the electronic-band wave functions are spread over the entire crystal. Mott[1,2] pointed out the crucial role of the electron-electron Coulomb repulsion in this process. The essential point of Mott's argument is contained in the following discussion. Given a collection of well-separated identical atoms each with a *single electron* outside a filled core (e.g., Na, etc.) in an *expanded* regular lattice, the energy required to remove an electron from a given site and place it elsewhere in the crystal is given by

$$\Delta E = I - A \quad , \tag{1}$$

where I is the ionization potential of the atom and A is the electron affinity (i.e., energy gained in forming the singly negative ion). A one-electron treatment of the atoms in question would of course lead to ΔE equal to zero. However, the existence of electron-electron Coulomb repulsion *on the atom* makes ΔE large and positive. One thus identifies ΔE with the Coulomb interaction U_0 between two electrons in the outer atomic orbital in question. The appropriate numbers for the hydrogen atom are $I = 13.6$ eV and $A = 0.5$ eV so that $U_0^{\mathrm{H}} = 13$ eV. Since the outer orbits of all atoms are approximately the same size, we may take this number as typical. It is precisely this Coulomb repulsion which keeps the electrons localized and prevents them from wandering about through the lattice in a band. Such localization, although advantageous insofar as the Coulomb interaction is concerned, is energetically costly in that if the electrons were allowed to delocalize into a band, the average one-electron energy would be lowered by an amount of order $\frac{1}{4}W$ where W is the bandwidth arising from the one-electron attractive potentials of the nuclei plus filled cores of the atoms in the solid. In a tight-binding theory, W is directly related to the transfer or hopping integral

$$T_{ij} = -\int \varphi_j^*(\vec{r}) H \varphi_i(\vec{r}) d^3r \quad , \tag{2}$$

where H is the total Hamiltonian for the system and where $\varphi_j(\vec{r})$ is a Wannier function which is localized about the jth nucleus at $\vec{R}_j$. The basic competition therefore is between the electron-electron Coulomb repulsion energy which tends to localize electrons and the band energy which tends to delocalize electrons.

However, the bare Coulomb interaction has long range; thus, for the electron transfer to occur, the energy given by Eq. (1) should actually be replaced by

$$\Delta E_{eff} = I - A - U_{0j} = U_0 - U_{0j} \equiv \Delta U , \tag{3}$$

where U_0 represents the repulsion between two electrons on the same site and U_{0j} represents that between two electrons on separated sites at R_0 and R_j, respectively.

In Mott's original paper,[1] he suggested that the change from localized (insulator) to band (metal) states would be catastrophic: a many-body phase transition. He argued that if one begins to make excitations of electron-hole pairs from the insulating ground state, the resulting free carriers can effectively screen the Coulomb interaction between other electrons, thus reducing the range of the interaction, and he predicted the existence of a first-order discontinuous phase transition. However, it seems evident that such screening effects, although important, can only be effective in reducing U_{0j} but can never significantly reduce the dominant on-site interactions U_0. Nevertheless, energetically a transition from insulator to metal will result as the atoms are brought closer together. There seem to be two dominant effects: (i) As the lattice constant is decreased the transfer integrals T_{ij} will increase in magnitude. The resulting increase in bandwidth favors the metallic state. (ii) As the lattice constant is decreased the near-neighbor Coulomb interactions increase in magnitude (toward U_0) again favoring the metallic state. One expects (i) to be the more important since the tails of the localized wave functions will vary exponentially with distance, while U_{0j} should vary more as d^{-1} where d is the lattice constant; but both effects must be taken into account.

Given a system with insulating ground state, one can expect a transition from insulator to metal with increasing temperature. Neglecting for the moment thermal-expansion effects, the argument is somewhat more subtle. Starting from zero temperature one expects an energy gap for the excitation of an electron-hole pair given approximately by Eq. (2). (The actual gap is reduced by finite overlap as described below.) However, having made a few e-h pairs, the electrons and holes are delocalized and free to move through the crystal. The result is that the creation of a subsequent excitation is made easier by the existence of the previously excited pairs. Energetically this would show up as a decrease in the magnitude of the energy gap, a renormalization of the gap toward zero, at which point the system is metallic. Doniach[3] argues that given N_e thermally excited e-h pairs, an electron going through the crystal experiences a random array of sites at which there is a hole. Averaging over the hole positions, the electrons see an average potential of $\Delta U(1 - N_e/N) = \Delta U(1 - n)$. Thus the average energy is given by

$$H_U^{av} = (\Delta U)n - \tfrac{1}{2}(\Delta U)n^2 \tag{4}$$

and the temperature (excitation) dependent gap is of the form

$$E_G(T) = E_G(0) - (\Delta U)n . \tag{5}$$

In Eq. (5), $E_G(0)$ may differ from ΔU because of finite overlap. Given Eq. (5) it is easy to see in a qualitative sense how the gap might renormalize with increasing temperature with an eventual transition to the metallic state. However, in addition to these average effects one must certainly include electron-hole correlations, particularly as the metallic state is approached. The physical point involved is the obvious tendency for electrons to correlate to stay apart in order to minimize the effect of the Coulomb repulsion. Such correlations give rise to the so-called "Coulomb hole"[4] in the metallic state. Coulomb correlations might well be expected to be the dominant effect in reducing the effective ΔU in the metallic state as well as in the insulating regime at relatively high temperatures where many excitations are present.

The nature of the proposed phase transition from insulator to metal has been the subject of considerable speculation. Mott originally argued for a first-order discontinuous transition, but in later papers[2] he suggested the possibility of second-order transition. Kohn[5] predicted a continuous change from semimetal to insulator via a series of "nested" transitions. The theoretical situation remains somewhat unclear. Experimentally insulator-to-metal transitions have been observed in a variety of transition-metal oxides.[6,7] In these cases the transition is usually highly first order with the conductivity changing by many orders of magnitude at the critical temperature. (Continuous transitions have also been observed; the case of SmB_6 is a prime example.)[8] However, the fact that large lattice distortions are often involved as well as the possibility of multiple bands playing a role[2] makes it difficult to say anything definitive in connection with the ideal transition discussed above.

A detailed theoretical description of the Mott insulating state and the M-I transition is not yet available. However, important progress has been made

by Hubbard[9] in an extensive series of papers. Hubbard has attempted to describe the relevant physics in terms of the model Hamiltonian

$$H = -t \sum_{\substack{\langle i,j \rangle \\ \sigma}} C_{i\sigma}^{\dagger} C_{j\sigma} + U \sum_{i} n_{i\uparrow} n_{i\downarrow} , \qquad (6)$$

where t represents the nearest-neighbor transfer integral between Wannier functions on neighboring sites in the lattice, U represents the Coulomb repulsion between two electrons on the same site, and $C_i^{\dagger}$, C_j, and n_i are the creation, destruction, and number operators for the localized Wannier states in question. Transfer integrals other than nearest neighbor are neglected. The Hubbard Hamiltonian, representing the simplest model that explicitly includes Coulomb repulsions, has been studied extensively in connection with the M-I transition, metallic ferromagnetism, and the general problem of Coulomb correlations in metals.[10] Equation (6) explicitly neglects the long-range Coulomb forces. However, one can perhaps view U in Eq. (6) as an effective interaction representing the Coulomb energy difference in making an excitation as given in Eq. (3), and we shall in fact take this point of view throughout this paper as discussed in Secs. III and VI. Hubbard[9] has shown the existence of a correlation energy gap in the excitation spectrum. Moreover, it is known that in the large Coulomb-interaction limit, the ground state is an antiferromagnetic insulator with exchange coupling between neighboring sites of order $2t^2/U$.[3] Various workers[11-14] have provided approximate treatments of the problem that suggest a phase transition to a metallic state as a function of temperature or pressure. However, the problem is far from solved.

Exact solutions of the Hubbard model are available for $T = 0\,^{\circ}\mathrm{K}$ in the somewhat simplified case of a one-dimensional system. The solution was first demonstrated by Lieb and Wu.[15] Ovchinnikov[16,17] was able to use their results to derive expressions for the single-particle energy gap and the spin-wave collective excitations. The direct relationship of the spin-wave dispersion relation to the zero-temperature susceptibility was pointed out by Takahashi.[18] These solutions and results are *exact* at $T = 0\,^{\circ}\mathrm{K}$ with respect to the model. Since the M-I transition seems to be conceptually difficult and since our understanding of these phenomena is so crucial, it is clear that an experimental system that approximates the one-dimensional Hubbard model would be of fundamental value. Such an experimental study of a system showing a Mott transition as a function of temperature and appearing to be an experimental realization of the one-dimensional Hubbard model is presented in this paper.

The localization of electronic wave functions from a single band by electron-electron interactions is not the only means of achieving a metal-to-insulator transition. Two other principal mechanisms have been proposed. The first was originally put forward by Peierls[19] and developed in detail by Adler and Brooks.[20] Peierls observed that a crystalline distortion would give rise to a lower symmetry with the result that additional one-electron band splittings would appear. If such splittings were to result in an energy gap at the Fermi energy, an insulating state would be obtained. This model was developed by Adler and Brooks[20] who included the lattice strain energy and worked out the thermodynamics for a narrow band model. The principal difference between the Mott insulator and the Adler-Brooks insulator is that the former is magnetic whereas the latter is a simple nonmagnetic state. The distinction becomes less clear if one allows the possibility of symmetry lowering because of an antiferromagnetic (AF) ground state.[21] However, if the insulating state were to arise from the AF symmetry, the M-I transition would always accompany the disordering of the magnetic system.

A second model was recently proposed and developed by Ramirez, Falicov, and Kimball.[22] They consider a system consisting of truly localized (e.g., $4f$) states plus a band at slightly higher energy and show that under appropriate conditions a metal-insulator transition will result. The importance of the spin entropy in the transition is emphasized in their model by associating the entropy change with the fact that in the two-band model the ionic configuration remaining after excitation of a carrier has higher spin than that before the excitation. As a result extra entropy is released thus favoring the transition. The entropy change in the case of the Hubbard model is less clear. However, a disordering of the AF ground state increases the entropy in the insulating phase and would appear to tend to inhibit the transition. The comparison which must be made is between the entropy in the insulating phase, which includes both spin disorder and single-particle excitations above the gap, and the band entropy in the metallic phase. This will be discussed in connection with experiment in Sec. VII.

II. WHY ORGANIC SOLIDS

This paper is concerned with an experimental study of an organic molecular solid. Such systems appear to offer unique opportunities for studies of phenomena that we traditionally associate with solid-state physics. The fundamental breakthrough in this area was the discovery of organic donor-acceptor radical-ion charge-transfer salts.[23] These salts represent the experimental realization of novel molecular compounds in which the ionization potential of the donor molecule I_D is relatively small and the electron affinity of the acceptor molecule A_A

is relatively large. The result is a charge-transfer salt with unpaired electrons appearing on the acceptor or donor, or on both. The existence of unpaired electrons in the highest occupied molecular orbitals allows such a system to be potentially a magnetic insulator[24] or a metal, [25,26] depending on the crystal structure, the strengths of the various interactions involved, and the temperature. The most interesting systems studied so far have been based on the acceptor molecule tetracyanoquinodimethan (TCNQ). [27] The fascinating molecular physics of this molecule will be discussed in detail in Sec. III. Here we wish to make some general comments on the use of organic systems in studying electronic phenomena in solids.

Given the existence of such charge-transfer salts, the organic molecular solids offer some unique advantages. Since only the lowest unfilled π molecular orbital (MO) of the acceptor is usually involved, one can hope to deal with a single-band system. This is to be contrasted with the presence of multiple bands in transition-metal oxides[6] where M-I transitions have been extensively studied. The multiple-band aspects of the problem, although interesting, certainly do not lead to a simplification.

Another advantage results from the usual flat planar structure of π molecular systems. Quite often the crystal structures[28] turn out to consist of simple linear chains of molecules stacked face to face. The resulting pseudo-one-dimensionality of the electronic structure is an essential simplification as well as being of interest in its own right. Moreover, since the typical radii of the π-electron wave functions ($2p_z$) are quite small compared to the observed intermolecular spacing, a tight-binding theory of the band structure should be adequate.

Use of organic molecules also provides means for reducing electron-electron Coulomb repulsions in solids. As mentioned above, a typical number for the Coulomb repulsion on an atom is of order 13 eV. This energy follows directly from confinement of the two interacting electrons in the region of order of the Bohr radius. From this point of view, molecules as fundamental units in a solid are particularly attractive, for their larger size makes possible a significant reduction of the effective Coulomb interactions. A further reduction of the effective Coulomb repulsion results from incorporating into the lattice large highly polarizable molecular cations which can in effect screen out Coulomb fluctuations. These points will be discussed in detail in Sec. III. The over-all result of the relatively weak intermolecular forces together with the small Coulomb interaction is the achievement of systems with U and W both of order 0.1 eV (10^3 °K). Under such circumstances, it is perhaps not surprising that relatively low temperatures are sufficient to drive the system from insulator to metal, etc. This is again to be contrasted with the situation expected for elemental compounds (e.g., transition-metal oxides) where both bandwidths and Coulomb interactions are of the order of a few eV. [6] With such large fundamental interactions it must be considered at best a fortuitous accident that temperatures of order 10^2 °K (0.01 eV) are sufficient to cause a major transition in the electronic structure.

Finally, the flexibility of organic chemistry toward producing molecules of desired structure and properties is quite clear. What is needed is an understanding of the molecular physics in sufficient depth to allow the design of properties on the molecular scale such that, when these molecules are put together into a crystalline solid, the resulting system will show solid-state properties of particular fundamental interest.

III. MOLECULAR PHYSICS OF TCNQ IN SOLID STATE

The TCNQ molecule is a closed-shell planar quinoid molecular having four highly electron-withdrawing cyanide groups located at the terminal methylene carbon atoms as shown in Fig. 1(a). These characteristics account for its very large electron affinity[27] and associated behavior of taking one electron when placed in contact with virtually any electron donor to form the open-shell $TCNQ^-$ monoanion radical. The single unpaired electron on $TCNQ^-$ occupies the lowest-energy empty π level and is expected to reside mainly localized on the terminal dicyano methylene carbon groups in order to take maximum advantage of the strong electron affinity of the cyanides. This picture of the electronic structure is confirmed by the theoretcial results of Lowitz, [29] by the small hyperfine coupling to the ring protons in solution studies, [30] and by analysis of the x-ray bond lengths associated with $TCNQ^-$. [31,32]

In the NMP-TCNQ salt, the positive charge resides in the σ structure of NMP primarily on the C and N atoms involved in the dative bond between the CH_3^+ group and the phenazine molecule [see Fig. 1(a)]. Thus the NMP cation is fully spin paired and should play no essential role in the physics of the NMP-TCNQ solid other than acting as a highly polarizable cation site.

X-ray studies of NMP-TCNQ[32] show a monoclinic structure consisting of linear chains of $TCNQ^-$ anions stacked essentially face to face. A diagram of the crystal structure is shown in Fig. 2. Similar parallel chains of NMP cations are found between TCNQ chains. The interplanar distance between TCNQ molecules within a given chain is 3.26 Å, whereas separation distances between TCNQ chains measured normal to a given TCNQ chain are 7.78 and 15.73 Å. Thus one expects the electronic structure can be described as pseudo-one-dimensional with maximum π-electron transfer

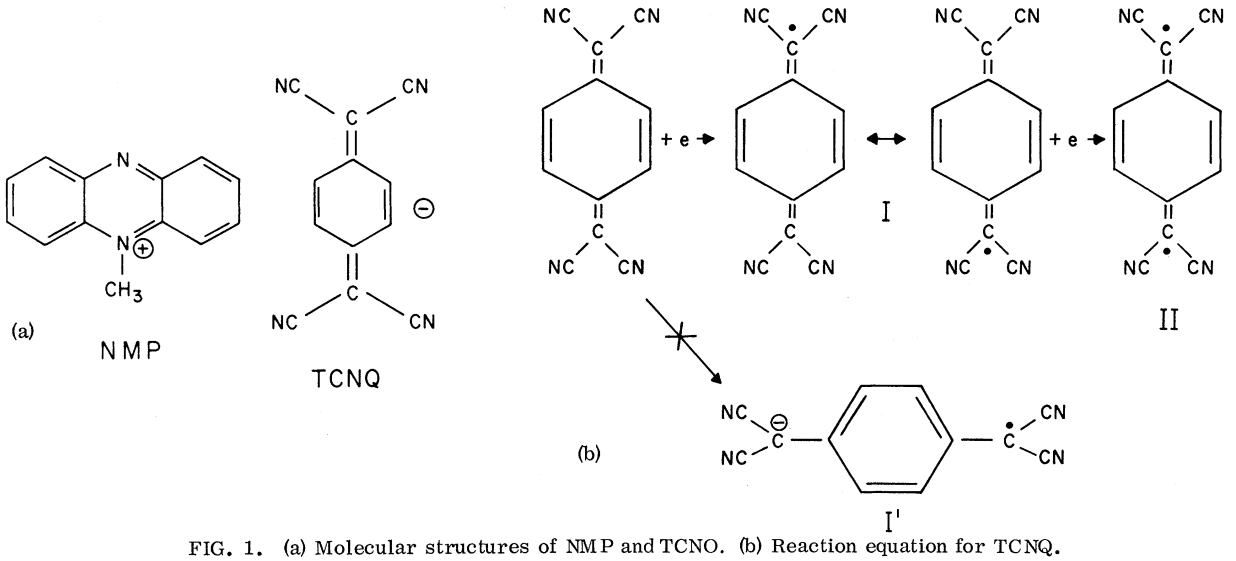

FIG. 1. (a) Molecular structures of NMP and TCNO. (b) Reaction equation for TCNQ.

occurring along the $TCNQ^-$ chain axis and nearly zero transfer otherwise. This tendency toward one dimensionality is enhanced by the directional nature of the $2P_z$ orbitals.

The energy required to transfer a single π electron in the solid from one $TCNQ^-$ site to an adjacent $TCNQ^-$ site depends on the effective Coulomb repulsion between the two odd electrons on the resulting $TCNQ^{--}$ dianion. The Coulomb repulsion between two outer electrons on a single C atom is about 10 eV.[33] However, on a $TCNQ^-$ site the characteristic separation distance can be greatly increased. Analysis of the bond lengths in the NMP-TCNQ x-ray structure shows the $TCNQ^-$ anion to be in the planar quinoid form (I) in agreement with theoretical expectations and not the canonical nonplanar benzenoid form (I') as shown in Fig. 1(b). We conclude that in the NMP-TCNQ salt, as well as the free $TCNQ^-$ ion, the excess charge density of $TCNQ^-$ resides primarily on the ends of the molecule where the one-electron attraction is greatest. In the event of an ionic fluctuation with *two* excess electrons on a single TCNQ molecule, there is a clear tendency for the two electrons to

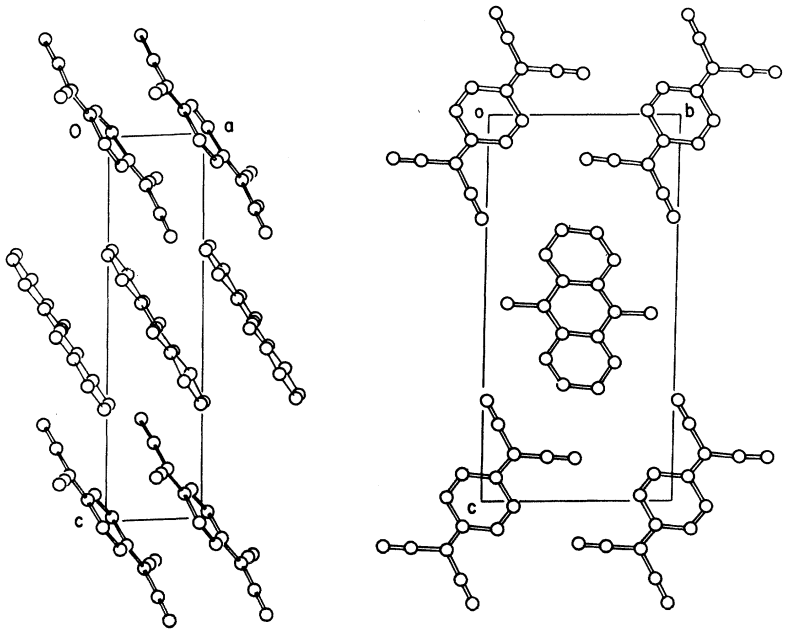

FIG. 2. X-ray crystal structure of NMP-TCNQ showing linear chains of $TCNQ^-$ anions stacked face to face with similar parallel chains of NMP cations between TCNQ chains (from Fritchie, Ref. 32).

localize at opposite ends of the molecule and correlate to stay apart in order to reduce their mutual Coulomb repulsion (II). This correlated structure may be schematically described by a generalized Heitler-London-type wave function[34]

$$\psi = \tfrac{1}{2}\sqrt{2}\,[\,\varphi_A(1)\,\varphi_B(2)+\varphi_A(2)\,\varphi_B(1)\,]\ , \qquad (7)$$

where φ_A denotes the wave function in the region of one dicyano methylene group (A) and φ_B denotes the wave function at the opposite group (B). As a result, when electron (1) is on group A, electron (2) is on group B, and vice versa. The characteristic distance now between electrons is 5.5–7 Å, so that the estimated Coulomb repulsion is drastically reduced to 2.0 – 2.5 eV. Allowing delocalization into the ring raises this energy somewhat. From semiempirical self-consistent-field molecular-orbital (SCFMO) theory, the value of U_0 has been estimated as[35,36] 3.5–3.9 eV. As in any self-consistent-field method, however, SCFMO theory probably underestimates the effect of electron correlation. Thus we estimate U_0 to be about 2.5–3.0 eV. The bare Coulomb repulsion U_1 between adjacent $TCNQ^-$ anions has been estimated as[36] 3.0 eV also using SCFMO charge densities for $TCNQ^-$. This too is probably somewhat of an overestimate for similar reasons. It seems likely, therefore, that the difference $U_0 - U_1$ is of the order of 0.5 – 1.0 eV. This value is confirmed by polarized optical-absorption spectra of K^+ $TCNQ^-$ of Hiroma *et al*.,[36] who find the associated charge-transfer band at 0.9 eV.

However, in the NMP-TCNQ solid, the energy involved in making the charge-transfer excitation ($U_0 - U_1$) should be significantly reduced as a result of the presence of the highly polarizable NMP cations in the nearby NMP chains. As pointed out by LeBlanc[37] this reduction is the result of induced electric dipoles on the NMP molecules in response to the electric fields resulting from the local charge fluctuation. The reduction is expected to be roughly by a factor of $(1 - \alpha/r^3)$ such that to a first approximation the effective interaction U_F would be given by

$$U_F \cong (U_0 - U_1)(1 - \alpha/r^3) = (U_0 - U_1)\eta\ , \qquad (8)$$

where α is the polarizability of NMP and r is the nearest distance between NMP and TCNQ. Values for r of about 5 Å require polarizabilities of about 100 $Å^3$ to reduce ($U_0 - U_1$) appreciably. Values for α of this order of magnitude for heterocyclic aromatic cations are not unreasonable.[38] Thus U_F might easily be reduced to a value of the order 0.1 eV in the NMP-TCNQ and related TCNQ salts containing polarizable cations. This mechanism of reducing U_F by cation polarizability is closely related to Little's indirect electron-electron interaction via polarizable side chains.[39] The reduced interaction introduced here can be thought of as arising from virtual excitons on the NMP chain, but the basic idea is quite similar. We shall see that a sizable reduction factor η is implied by experimental studies of the NMP salt.

Experimental measurements independent of those reported below are available that suggest U_F may indeed take on values as low as 0.1 eV. The polarographic half-wave potentials $\epsilon_{1/2}$ of the single-electron reactions[27]

$$TCNQ^- \rightarrow TCNQ^0 + e\ , \qquad (9a)$$

$$TCNQ^- + e \rightarrow TCNQ^{--} \qquad (9b)$$

measured in the highly polar solvent CH_3CN, are +0.129 and −0.294, respectively. The energy change for the reaction $2TCNQ^- \rightarrow TCNQ^0 + TCNQ^{--}$ is given by

$$\Delta E_{1/2} = \epsilon^{-}_{1/2} + \epsilon^{--}_{1/2} = 0.16 \text{ eV}\ , \qquad (10)$$

where the superscripts (−) and (− −) denote the reactions (9a) and (9b), respectively. The energy contribution in this case that reduces U_0 is usually denoted as the solvation energy ΔE_s,[40] such that

$$U_0 = \Delta E_{1/2} + 2\Delta E_s\ , \qquad (11)$$

$$U_{eff} = \Delta E_{1/2} = U_0 - 2\Delta E_s\ . \qquad (12)$$

Values of ΔE_s have been estimated for aromatic hydrocarbon anions by Hedges and Matsen[41] to be in the range 1–4 eV, which are quite adequate to reduce U_0 of several eV to a U_F of tenths eV. That this difference in half-wave potentials for $TCNQ^-$ imbedded in a highly polarizable cavity is similar in the two cases is not unreasonable. The polar liquid in solution, roughly speaking, plays the role of the cation polarizability in the solid. We note in addition that the half-wave potentials can be used to obtain information on the *relative* magnitude of U_0 for different molecules provided the same solvent is used for comparative measurements. Thus, polarographic studies are useful for determining likely candidates for organic metals.

IV. EXPERIMENTAL TECHNIQUES

The tetracyanoquinodimethan (TCNQ) was prepared following the procedure of Melby *et al*.[27] The resulting material is believed to be the best reported to data, since recrystallization from Ar-bubbled acetonitrile (MCB chromato-quality grade) resulted in crystalline yellow-orange material which when viewed under a microscope was found to be composed of bright yellow well-formed crystals. The TCNQ gave brilliant yellow-orange solutions when dissolved in Ar-bubbled acetonitrile. TCNQ was originally reported[27] as a rust-brown powder giving yellow to yellow-green acetonitrile solutions. NMP-TCNQ was prepared according to Melby[42] from NMP methosulfate (Aldrich Chem-

ical Co.). All elementary chemical analyses were carried out in duplicate by Galbraith Laboratories, Knoxville, Tenn. The analyses for samples used in the experiments in every case indicated stoichiometry with correct elemental composition to within the experimental error. Each NMP-TCNQ powder sample was compacted into pellet form for specific-heat determination immediately upon completion of the magnetic-susceptibility measurement. Single crystals, where used, were obtained by recrystallization from solution.

The classic techniques for measuring magnetic susceptibility (Faraday, Gouy, and Foner methods) measure the total susceptibility of a bulk sample. In general,

$$\chi_{tot} = \chi_n + \chi_e + \chi_d \ , \tag{13}$$

where χ_n is the static nuclear paramagnetic susceptibility, and χ_e and χ_d are the static electron paramagnetic and diamagnetic contributions, respectively. χ_d includes the diamagnetism of the inner valence shells of atoms, ions, and molecules, and the orbital diamagnetism of conduction electrons. For most situations the nuclear contribution is much less than that of the electrons, and χ_e and χ_d are often of the same order of magnitude, making it very difficult to separate their contributions. To deduce χ_e from χ_{tot}, χ_d may be *estimated* using Pascal's constants[1] and subtracted from χ_{tot}.

Using the technique of Schumacher and Slichter[43] it is possible to measure χ_e directly and thus avoid the ambiguities inherent in the classical techniques. Qualitatively, the technique is to perform electron and nuclear (proton) paramagnetic resonance on a sample at a constant frequency, changing only the applied field by three orders of magnitude. The areas under the recorded absorption curves (A_e and A_p) are proportional to the electron and proton spin magnetizations, the constants of proportionality for the electron and proton resonances differing only by known changes in amplifier and modulation settings. Defining these constants as K_e and K_p for the electron and proton resonance, respectively, K_e equals cK_p. It is obvious that c involves only easily calibrated amplifier settings because in going from electron to nuclear resonance or vice versa, only external field, amplifier, and modulation settings are changed, leaving the rf (30 MHz), rf level, circuit Q, and sample skin depth constant. Taking ratios of the recorded areas, we have

$$\frac{A_e}{A_p} = \frac{k_e M_e}{K_p M_p} = \frac{c k_p \chi_e H_e}{K_p \chi_p H_p} = \frac{c H_e}{\chi_p H_p} \chi_e \tag{14}$$

or

$$\chi_e = \frac{1}{c}\left(\frac{H_p}{H_e}\right)\left(\frac{A_e}{A_p}\right)\chi_p \ , \tag{15}$$

where H_e and H_p are the external applied resonance fields for electrons and protons, respectively. χ_p is the static proton susceptibility which can be calculated exactly from a Curie law. Since the technique is basically a resonance experiment, contributions to χ_e which do not involve angular momentum (e.g., the Van Vleck temperature-independent susceptibility) will be specifically excluded.

Phase-sensitive detection was used to observe the derivative of the absorption curves, care being taken to prevent over modulation and saturation of the signals. The components of the spectrometer used are shown in Fig. 3. As a marginal oscillator responds only to absorption χ'' (the dispersion producing only a slight frequency shift) a true measure of static susceptibility is obtained. The curves were automatically digitized and then integrated by computer. Figure 4 shows the typical digital data.

The NMR curves, being almost Gaussian in shape, presented little difficulty. Having established the temperature independence of the apparatus sensitivity, the NMR curves were integrated only at low temperatures to obtain a calibration. The ESR curves, being approximately Lorentzian in shape, require a more extensive analysis. Because of finite signal to noise it was possible to integrate only part way into the wings of the Lorentzian derivative line. To properly account for this, all ESR curves were integrated to the same relative position in the wings (integration was carried out with limits of seven times the peak-to-peak linewidth on either side). This technique underestimates the size of the electron resonance absorption by a constant percentage, characteristic of the line shape. The results of the numerical quadrature were therefore averaged with that of an

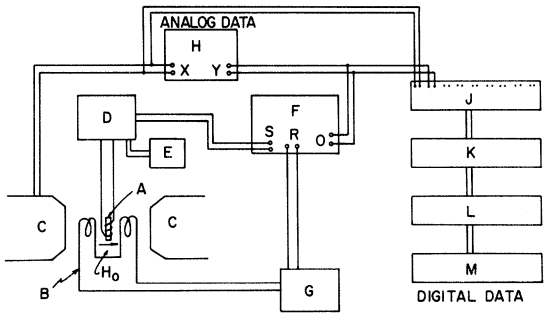

FIG. 3. Electron-spin-resonance spectrometer: (A) sample, (B) field modulation coils, (C) electromagnet, (D) marginal oscillator, (E) frequency meter, (F) lock-in amplifier [(S) signal, (R) reference, (O) output], (G) audio amplifier, (H) x-y recorder (analog data output), (J) multiplexer, (K) analog-to-digital converter, (L) parallel to series converter, (M) Teletype (digital data output). H_0 is the applied magnetic field.

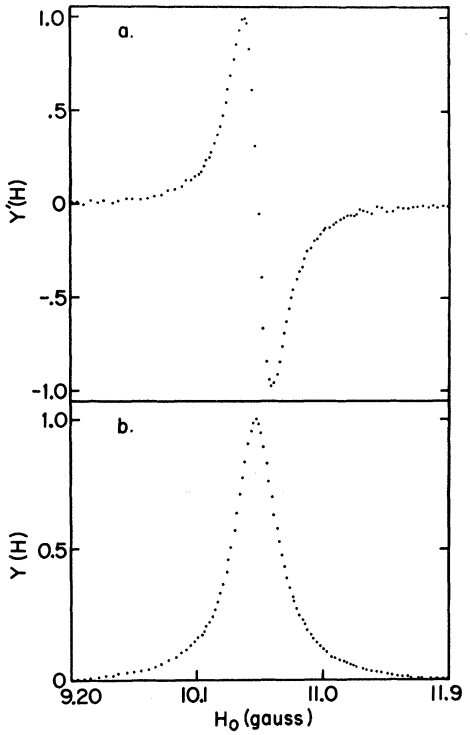

FIG. 4. (a) Typical digitized ESR derivative signal ($T = 2.89$ °K), plotted in relative units vs applied magnetic field (in gauss). (b) Plot of absorption (relative units) vs applied field obtained by numerical integration of the curve in part (a). The ratio of the full linewidth at half-amplitude of the absorption curve to the peak-to-peak linewidth of the derivative curve is 1.73, exactly what is expected for a Lorentzian curve.

ideal Lorentzian of the same linewidth in order to estimate the true absorption (e.g., a correction factor of 9% was used). Using these techniques, the reproducibility of the measured susceptibility for different samples was found to be plus or minus 3%.

The heat-capacity measurement on NMP-TCNQ utilized a standard continuous heating and drifting technique. The calorimeter is schematically drawn in Fig. 5. The sample is a compacted pellet and is placed between the two smooth faces of the sample holder (SH) using a small amount of Apiezon grease for thermal contact. The sample holder has two parts: The lower part is hung by three silk strings (SS) from the frame (F) and carries the heater (H) as well as the phosphor bronze heat conductor (MS) of the mechanical heat switch. The upper part of the sample holder carries a germanium resistance thermometer (T) and is attached to a screw assembly (SA) by additional silk threads. By turning the screw one can squeeze tight on the sample.

The frame carries an auxilliary heater (AH) which can be adjusted manually to minimize the heat loss through electrical leads. On top of the frame are thermally anchored but electrically isolated copper studs (TA) which provide the connection between incoming copper leads (CL) and the superconducting electrical leads (SC) to the thermometer and heater. The entire frame is in turn hung by silk threads from a thermal station (TS). If necessary one can maintain a large temperature difference between the sample and the bath by introducing another auxilliary heater at this point. A nylon screw (NS) joins this thermal station to the brass top flange (TF).

The mechanical heat switch uses a bellows assembly (BA) which can be lowered or raised from the outside. An indium covered copper heat sink (CS) is attached to the bottom of the bellows. By lowering the bellows, the head conductor (MS) is pressed against the switch base (SB) making the thermal contact.

The specific heat is measured by introducing a known amount of heat ΔQ and measuring the corresponding temperature change ΔT_R as a function of time. In order to compensate for thermal drift due to vibration, radiation, and residual thermal contact, the temperature is monitored during the drift cycle before and after each heating cycle. By observing the temperature change in these two

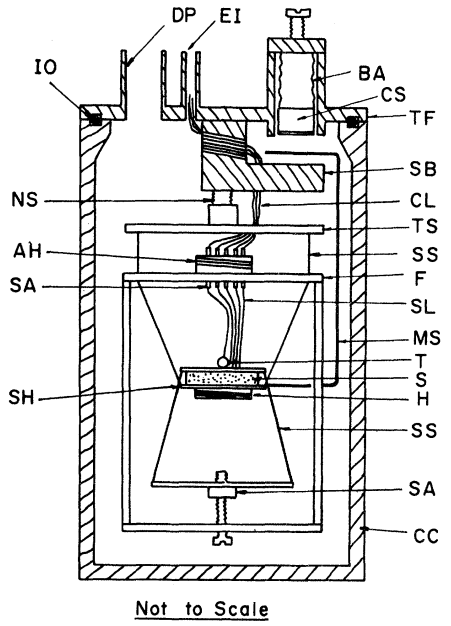

FIG. 5. Specific-heat cryostat: (AH) auxilliary heater, (BA) bellows assembly, (CC) calorimeter can, (CL) copper leads, (CS) copper sink, (DP) diffusion pump, (EI) electrical inlet, (F) frame, (H) heater, (IO) Indium O-ring, (MS) mechanical switch, (NS) nylon screw, (SA) screw assembly, (S) sample, (SB) switch base, (SH) sample holder, (SL) superconducting leads, (SS) silk string, (T) thermometer, (TF) top flange, (TS) thermal station.

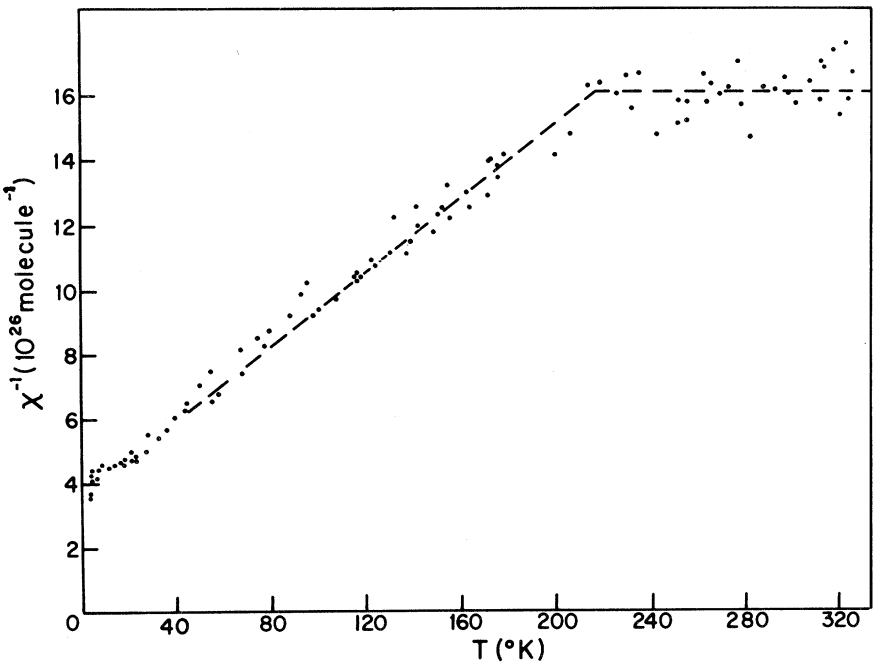

FIG. 6. Inverse electron *spin* susceptibility per molecule vs temperature for NMP-TCNQ.

drift cycles one can calculate the correction ΔT_c due to drift. The net temperature change due to the measured heat input is, therefore, $\Delta T = \Delta T_R - \Delta T_c$, and the average specific heat over the interval ΔT is then $\overline{C} = \Delta Q/\Delta T$.

The low thermal conductivity of the organic samples requires the use of long drift periods and slow heating in order to assure thermal equilibrium. As a result, an attempt was made to minimize the unwanted heat input due to vibration, etc. For vibration isolation the Dewar assembly was placed at the center of a 1-ton triangular-base concrete prism which was in turn supported on three air springs.

The data were taken in digital form. The system was fully automated with the timing of the heating and drifting periods as well as the sampling times controlled by a standard oscillator and a set of scalars. To measure the temperature change and the drift, ten temperature points were taken during each 250-sec heat or drift period. The thermal relaxation time of the measured samples was estimated from the temperature-vs-time profile to be about 50 sec. This was taken into account in the subsequent data analysis. The sample-holder contributions were separately measured so that the data analysis by computer gives directly the sample specific heat.

V. EXPERIMENTAL RESULTS

A preliminary account of the experimental results obtained for the NMP-TCNQ system has been published elsewhere.[44] Analysis of the susceptibility and specific-heat data aided by the temperature dependence of the electrical conductivity yields a picture of a transition from metal (above 200 °K) to small band-gap magnetic insulator at lower temperatures. The low-temperature properties are in quantitative agreement with the predictions of the one-dimensional Hubbard model.

The temperature dependence of the electron *spin* susceptibility is shown in Fig. 6 plotted as χ^{-1} vs T. We emphasize once again that the resonance technique utilized gives the spin susceptibility directly; diamagnetic and Van Vleck temperature-independent contributions to the total bulk susceptibility are specifically excluded. Above 200 °K, the susceptibility is relatively small (6.2×10^{-28} per molecule) and temperature independent. Since the conductivity (Fig. 7)[45] is large and shows a negative temperature coefficient above 200 °K, it is natural to associate this high-temperature region with the metallic phase. Further corroboration is found in the thermoelectric power (TEP) measurements of Buravov *et al.*[46] (Fig. 7). Above 200 °K, the TEP is small and negative, and has a linear temperature dependence with negative slope characteristic of a metallic system. Thus the high-temperature susceptibility is, in fact, the Pauli spin susceptibility of the interacting metallic electrons. The value of 6.2×10^{-28} per molecule corresponds to a density of states of 5.8 states eV^{-1} molecule^{-1} using the simple expression for the Pauli susceptibility:

$$\chi_{\text{Pauli}} = 2\mu_B^2 \rho(0) , \tag{16}$$

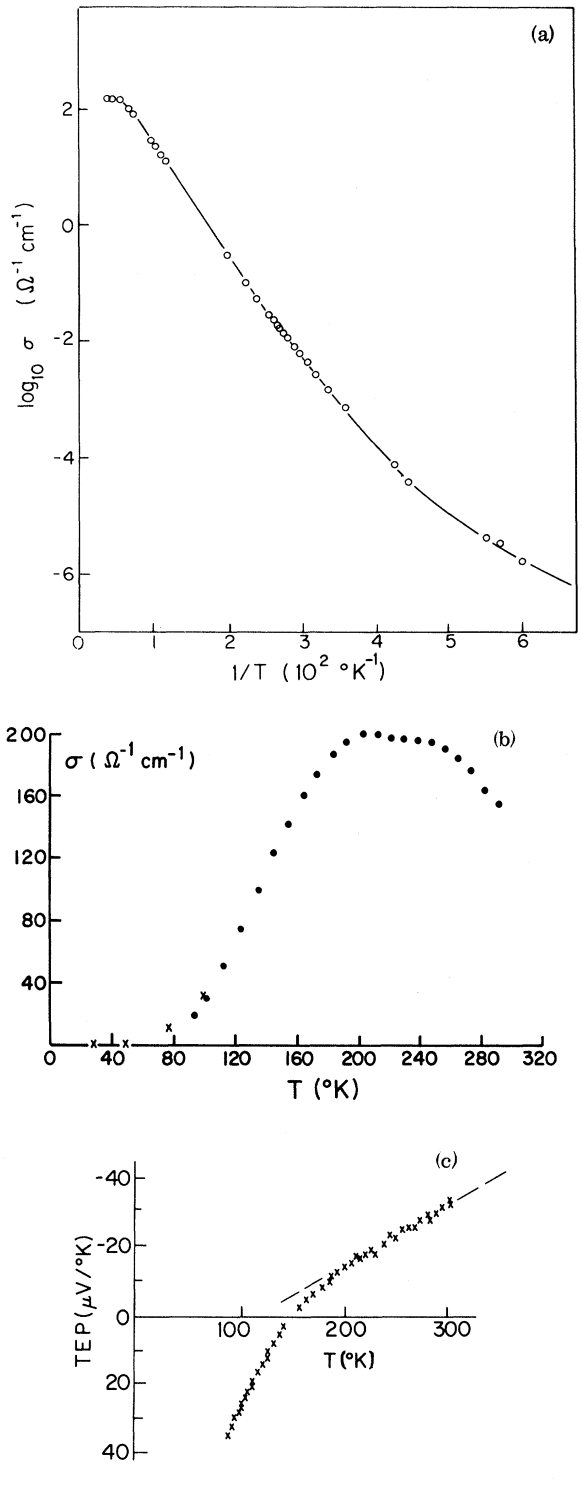

FIG. 7. (a) Temperature dependence of the conductivity for single crystals of NMP-TCNQ (from Ref. 45). (b) Conductivity vs temperature for NMP-TCNQ showing the high-temperature behavior in more detail. Low-temperature points (×) are from Ref. 45, the higher-temperature points were obtained from crystals prepared in our laboratory. (c) Thermoelectric power (TEP) vs temperature for single-crystal NMP-TCNQ (from Ref. 46).

where $\rho(0)$ is the band density of states for a single sign of spin. Equation (16), however, neglects electron-electron interactions. Including the short-range (δ function) repulsion as in the Hubbard model, the standard random-phase-approximation (RPA) (Hartree-Fock) result may be written[47]

$$\chi = 2\mu_B^2 \frac{\rho(0)}{1 - U\rho(0)} \quad , \tag{17}$$

where U is the Coulomb repulsion. From a single susceptibility measurement one cannot tell if enhancement effects are important. We shall return to this in Sec. VI where the analysis will be given which indicates little or no enhancement of the Pauli susceptibility in the metallic phase.

Below 200 °K, there is a broad range of temperatures in which the susceptibility follows a Curie-Weiss law

$$\chi = C/(T + 0) \quad , \tag{18}$$

where $\theta = 61$ °K, and the Curie constant $C = 1.7 \times 10^{-25}$ °K per molecule. Using the standard expression for the Curie constant

$$C = N\,(p_{eff}^2\,\mu_B^2/3K_B) \, , \tag{19}$$

one finds an effective moment $p_{eff} = 0.9\mu_B$. Our interpretation therefore is that below 200 °K the system is at least partially described as an ensemble of disordered paramagnetic "localized moments." For a fully formed spin-one-half system one expects $p_{eff} = \sqrt{3}$, a value considerably larger than that obtained from the experimental slope of χ^{-1} vs T. We emphasize that the linearity of χ^{-1} vs T persists over a factor-of-5 change in temperature so that the magnitude of the effective moment is apparently constant throughout this interval. In the vicinity of 200 °K, the moments go away as the system goes over into the metallic state. The transition is gradual (see the conductivity in Fig. 7), but over a region of not more than $\Delta T \sim 30$ °K the susceptibility evolves from the Curie-Weiss form with constant p_{eff} to an essentially temperature-independent Pauli contribution.

The existence of disordered localized moments is consistent with the picture of the metal-insulator transition, driven by Coulomb correlations which prefer one electron per site with minimal double occupancy fluctuations. The general arguments given in Secs. I and III suggest that if U_F is large enough, a gap appears resulting in a low-temperature magnetic state for the system. Clearly, as $U_F/t \to \infty$ there will be exactly one electron per site. In this limit one expects $p_{eff} = \sqrt{3}$ as described above. The experimental results thus imply a system with intermediate coupling strength; U_F is large enough to localize the electrons into a low-temperature magnetic insulating state, but not large enough to achieve the maximum value of spin one-

half per site.

Let us carry this argument one step further. The constant slope of χ^{-1} from 40–180 °K was used above as an indication of localized moments with a constant p_{eff}. Since the size of the magnetic moment is directly related to the strength of the Coulomb interaction, this result may be used to infer that the renormalization effects on U_F discussed in the Introduction are relatively unimportant at least until the temperature approaches close to the metal-insulator transition temperature.

In the relatively large U_F limit which seems to be important here, there are basically two energies in the problem: (i) U_F, the effective Coulomb interaction which forms the moments, and (ii) $2t^2/U_F$, the transfer antiferromagnetic (AF) exchange energy between localized moments. The latter is a perturbation-theory result[3] based on the zeroth-order picture of the ground state as having one localized spin per site in which the energy is lowered by allowing virtual charge transfer onto neighboring sites. Because of the one-orbital nature of the problem, the energy lowering appears only if neighboring spins are antiparallel; hence (ii) may be thought of as an antiferromagnetic exchange interaction.

The experimental evidence of antiferromagnetism at low temperatures is twofold. First, the extrapolated Curie-Weiss θ of 60 °K implies the existence of antiferromagnetic interactions. Equally important however is the observed rounding off of χ to a constant value below 30 °K. This is qualitatively as expected for a 1d AF system. The rapid downturn of χ^{-1} below 10 °K is the result of impurities. From the magnitude of the contribution one can estimate the impurity content as about 0.2%. This low impurity level is crucial in obtaining the correct picture of the behavior of the sample susceptibility at low temperatures.[45] The samples used in the susceptibility experiment were in the form of powders. This would present possible difficulty were it not for the fact that the system in question is essentially one dimensional and made entirely of first-row elements. Consequently anisotropy effects are negligible, and the measured χ may be regarded as a perpendicular susceptibility. This will be discussed in more detail in connection with the dynamics of the resonance in Sec. VIII.

From the susceptibility results we therefore conclude the following: (i) There is a metal-insulator transition at approximately 200 °K. (ii) The system cannot be treated in the strong-coupling limit, for a reduced effective moment is observed in the paramagnetic state. (iii) The local moments "turn on" relatively quickly with decreasing temperature below 200 °K, and remain at fixed magnitude as the temperature is lowered. (iv) The ground state is an antiferromagnetic insulator. (v) The fact that two transitions are observed (a Mott transition at 200 °K and an AF transition at 30 °K) implies $U_F/t > 1$. *Note that the word "transition" is used in a qualitative sense throughout this paper. There are no sharp phase transitions in this one-dimensional system.*[48]

To investigate the low-energy elementary excitation spectrum in the AF state we have measured the low-temperature specific heat of NMP-TCNQ. One expects that the predominant electronic excitations (i.e., neglecting phonons and molecular vibrations and rotations, etc.) will be spin waves. The existence of the unshifted electron spin resonance signal ($k = 0$) indeed implies zero gap for the spin-wave spectrum. Thus one naively expects the spin-wave spectrum with linear dispersion relation characteristic of antiferromagnetic systems.[49,50] The experimental results are shown in Fig. 8 plotted as C/T vs T^2. Below 4.2 °K, the specific heat can be represented as

$$C = \alpha_M T + \beta T^3 \quad , \tag{20}$$

where $\alpha_M = 1.9 \times 10^3$ erg/°K g and $\beta = 5.6$ erg/°K^4 g. The T^3 term is the expected Debye lattice contribution and implies a Debye temperature of $\Theta_D = 90$ °K. The linear term we associate with the spin-wave contribution. We emphasize that the data of Fig. 8 cover a temperature range of 1.8–4.2 °K where the system is insulating with a resistivity greater than 10^6 Ω cm. Thus the linear term is in no way connected with the γT term expected for an electron gas.

A specific-heat contribution linear in T for an AF system implies that the system in question may be regarded as one dimensional insofar as its electronic excitation spectrum is concerned. (Of course, the macroscopic lattice is three dimensional, and the phonon restoring forces, although anisotropic, average at low temperatures to give a three-dimensional Debye lattice contribution.) The argument is straightforward. Assuming the spin waves are bosons, their contribution to the internal energy is

$$\overline{E} = \sum_k \frac{\epsilon_k}{e^{\beta\epsilon_k} - 1} \Rightarrow \int dk \frac{\epsilon_k}{e^{\beta\epsilon_k} - 1} \quad , \tag{21}$$

where $\epsilon_k = \hbar V_s k$ is the (low-k) dispersion relation and $\beta = 1/k_B T$. Thus, changing variables, we have

$$\overline{E} \sim \frac{1}{\beta^2 \hbar V_s} \int_0^\infty \frac{x\,dx}{e^x - 1} \sim \frac{k_B^2 T^2}{\hbar V_s} \quad . \tag{22}$$

The resulting specific heat is linear in T with a coefficient depending inversely on the spin-wave velocity. For two and three dimensions the integral in Eq. (22) is correspondingly modified, yielding the general result that the spin-wave contribution is proportional to T^d where d is the dimensionality.

The experimental fact that the system can be re-

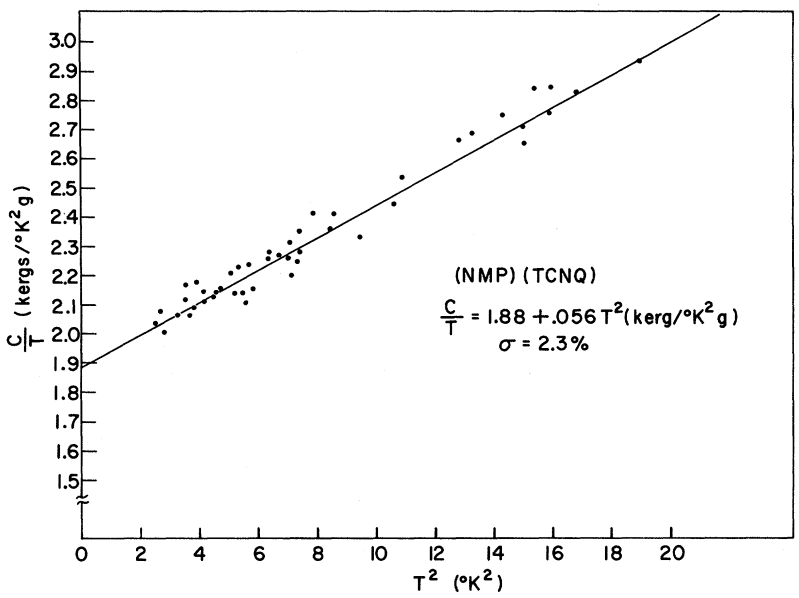

FIG. 8. Specific heat per gram of NMP-TCNQ in the low-temperature insulating phase. Data are plotted as c/T vs T^2.

garded as one dimensional is remarkable. Although, as discussed above, the lattice structure lends itself to a one-dimensional point of view, that interchain transfer matrix elements are truly negligible is an important and simplifying result. The essential point is evidently the directional nature of the p_z orbitals which make up the π system of the TCNQ molecule together with the chainlike structure.

Since long-range order cannot exist in a one-dimensional system,[48] one might question an analysis in terms of spin waves. Such arguments are unjustified, for recent experimental and theoretical work has clearly demonstrated the existence of spin waves in one dimension.[51–54] The inelastic neutron data of Birgenau *et al.*[52] for the system $(CH_3)_4\,NMnCl_3$ give direct evidence of spin waves. Moreover, Blume, Watson, and Vineyard[52] have shown that chains consisting of as few as 30 spins are sufficient to show collective spin-wave excitations, and the numerical calculations of Bonner and Fisher[53] independently indicate a linear temperature dependence to the specific heat. The specific-heat results presented here thus provide further evidence, and in fact suggest that such spin waves contribute to the thermodynamic properties in a relatively straightforward manner. The specific-heat results thus represent one of the first observations of the linear temperature dependence predicted for the one-dimensional antiferromagnet.

One might argue that the insulating state described above is the result of the well-known Peierls instability of one-dimensional systems to small lattice distortions. This is particularly important for narrow bands as shown by Adler and Brooks. That this is not the case for NMP-TCNQ is demonstrated by the magnetic character of the insulating phase. Although the existence of a small lattice distortion belwo 200 °K cannot be ruled out without x-ray data on the temperature dependence of the structure, the magnetic properties of the low-temperature phase imply that the insulating state results from Coulomb correlations, i.e., the system is a Mott insulator. One further comment is in order. The ordinary thermal expansion of the crystal with increasing temperature tends to increase the lattice constant and thereby decrease the transfer integral slightly. Thus, the effect of thermal expansion is to favor the insulating state; it does not drive the transition from insulator to metal.

VI. ANALYSIS OF LOW-TEMPERATURE RESULTS

The low-temperature magnetic susceptibility and specific-heat results presented above can be analyzed in terms of the one-dimensional Hubbard model with one electron per TCNQ site.[54] When attempting to justify the application of such an idealized model to a real physical system, two questions arise. First, is the NMP-TCNQ system truly one dimensional? We have argued this point above; the lattice structure together with the linear (in T) term in the specific heat appears to provide adequate evidence. Second, is it reasonable to represent the Coulomb interactions in a real system in terms of a single parameter as in the Hamiltonian of Eq. (6)? It was shown in Sec. I that the energy involved in making a charge-transfer excitation is [see Eq. (3)]

$$\Delta U = U_0 - U_{0j}\,, \tag{23}$$

where U_{0j} is the long-range Coulomb interaction between two electrons, respectively, on sites 0 and j. There are two simplifying features. In the me-

tallic state, where the electrons are free to move, one can expect screening effects to make the long-range interactions negligible. Note that although the electronic structure is one dimensional, the parallel chains exist in a microscopic crystal so that three-dimensional metallic screening should be effective in reducing non-nearest-neighbor interactions. Moreover, Kuper[55] has considered metallic screening in pseudo-one-dimensional configurations with characteristic cross-sectional diameters of several angstroms. The cross-sectional diameter of a linear TCNQ chain in NMP-TCNQ may be considered as the molecular dimension 7 Å which according to Kuper's treatment results in a screening length of order one lattice constant. In the insulating state a small energy gap appears reducing the screening response. In this limit, the electronic system has the properties of a dielectric medium with dielectric constant[56]

$$\epsilon \sim 1 + \omega_p^2/\omega_G^2 \ , \tag{24}$$

where $\omega_p^2 = 4\pi Ne^2/m$ is the plasma frequency and $\hbar\omega_G = E_G$. Although Eq. (24) was derived assuming E_G resulted from a single-particle band gap,[56] the essential point is the existence of a finite energy for making charge-transfer (ionic) excitations. If ω_G is small, one can expect a large dielectric constant in the insulating phase. The experimental value for the dielectric constant of NMP-TCNQ at low temperature has been measured by Buravov *et al.*[57] who find $\epsilon \sim 400$. Thus using metallic screening and large dielectric constant in the two appropriate regimes, one concludes that *long-range effects can be neglected.* We shall therefore assume the effective interaction to be dominated by U_0 when the two electrons are on the same molecule, and U_1 when the two electrons are on nearest-neighbor molecules, all other interactions being negligible. Thus we have

$$U_F = (U_0 - U_1)\eta \ , \tag{25}$$

where $\eta \simeq (1 - \alpha/r^3)$ is the cation polarizability reduction factor introduced in the discussion of Sec. III. For the much simpler problem of a two-atom chain Falicov and Harris[58] have explicitly shown that inclusion of both on-site and nearest-neighbor Coulomb repulsion can be rigorously represented in terms of a simple Hubbard Hamiltonian of Eq. (6) with U_F taking the form of Eq. (25) (with η in this case being obviously unity).

The exact zero temperature solution of the half-filled one-dimensional Hubbard model [Eq. (6)] was first demonstrated by Lieb and Wu.[15] Ovchinnikov[16,17] has developed the solution in considerable detail deriving expressions for the dispersion relations for single-particle as well as collective (spin-wave) excitations. The Ovchinnikov single-particle excitation spectrum is sketched in Fig. 9 in the limit where $U_F/t \gg 1$. One sees an electron band and a hole band separated (at $k = 0$) by the Coulomb interaction U_F. The electron and hole bands are of the form $\epsilon_k = t\cos ka$, where a is the lattice constant. As a result the excitation spectrum for taking an electron from k and putting it in $k+q$ is given by (again in the limit $U_F/t \gg 1$)

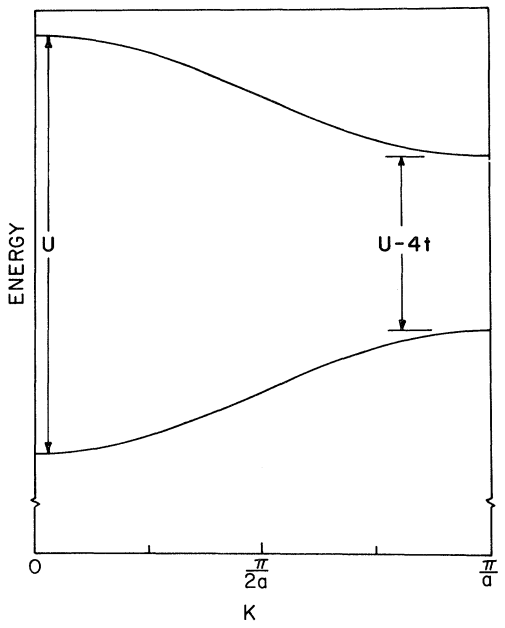

FIG. 9. Exact single-particle excitations for the one-dimensional Hubbard model as derived by Ovchinnikov (Refs. 16 and 17). The drawing is appropriate only to the strong-coupling limit of $U_F/t \gg 1$.

$$E_k(q) = U_F + t[\cos(k+q)a + \cos ka] - 2t \ . \tag{26}$$

The minimum energy gap occurs at $k = \pi$, $q = 0$ so that the Hubbard gap has the limiting form ($U_F/t \gg 1$)

$$E_H = U_F - 4t + \cdots \ . \tag{27}$$

Equation (27) is approximate; the exact result valid for all values of the parameters was derived by Ovchinnikov[16]

$$E_H(x) = \frac{16t^2}{U_F}\int_1^\infty \frac{(y^2-1)^{1/2}dy}{\sinh xy} \ . \tag{28}$$

The Hubbard gap as computed from this equation is plotted numerically in Fig. 10 as a function of the variable $x = 2\pi t/U_F$. One sees the two limiting forms: For $U_F/t \gg 1$, Eq. (27) is valid, whereas for $U_F/t \ll 1$, the Ovchinnikov result is

$$E_H \simeq (8/\pi)(tU_F)^{1/2} e^{-2\pi t/U_F} \ . \tag{29}$$

The latter result is reminiscent of the spin-density wave solution expected for such a system as a re-

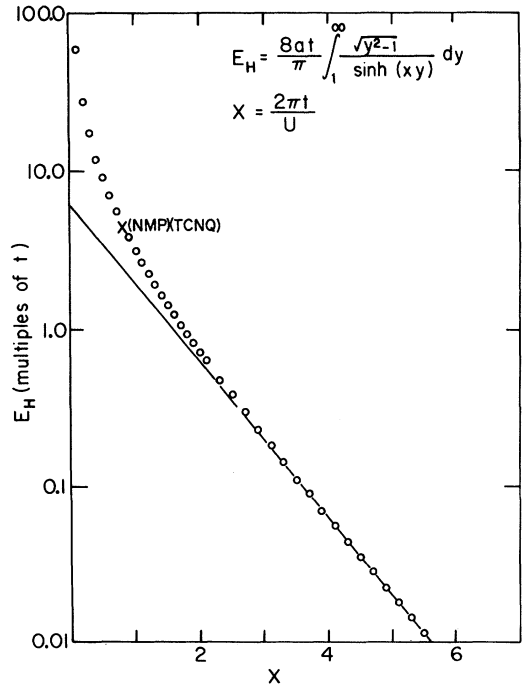

FIG. 10. Hubbard gap as a function of $x = 2\pi t/U_F$. The open circles are computed numerically using the Ovchinnikov expression [Equation (28) of the text]. The solid line indicates the *weak*-coupling limit of Eq. (29). Value of E_H appropriate to NMP-TCNQ is indicated.

sult of the divergence in $x(q)$ at $q = 2k_F$ for a one-dimensional metal.

The nonanalytic form of the energy gap in the small interaction limit is of interest from another point of view. Lieb and Wu[15] state that there is no Mott transition for the one-dimensional Hubbard model at $T = 0\,^\circ$K. Their statement rests on the fact that for arbitrarily small U, the single-particle gap is finite. However, in contrast to their assertion in the paper, Eq. (29) shows the resulting gap to be a nonanalytic function for small U.[59] This strongly suggests by analogy with other many-body phenomena[60] that when k_BT is of order the Hubbard gap, the system will go over into the metallic state. This is discussed in more detail in Sec. VII.

In addition to the single-particle charge-transfer excitations the collective spin-wave modes are included in Fig. 11. The precise form for the spin-wave dispersion relations again depends on the value of U_F/t; the sketch in Fig. 11 is drawn for a value of U_F/t appropriate to NMP-TCNQ.

Takahashi[18] has derived an expression for the zero-temperature magnetic susceptibility using the Lieb and Wu solution

$$\chi(0) = 2\mu_B^2\,(Na/\pi\hbar V_s)\ . \tag{30}$$

The parameter V_s has the dimensions of a velocity and is given by

$$V_s = \frac{2at}{\hbar}\,\frac{I_1(x)}{I_0(x)}\ , \tag{31}$$

where I_0 and I_1 are modified Bessel functions of the argument $x = 2\pi t/U_F$. Takahashi observed that the velocity V_s is precisely the spin-wave group velocity as derived by Ovchinnikov:

$$\left|\frac{d\epsilon^s(q)}{dq}\right| = \hbar V_s \quad (q \to 0, \pi)\ . \tag{32}$$

This definite numerical relation between $\chi(0)$ and the spin-wave dispersion relation has been used as a numerical check on the validity of the model to the NMP-TCNQ system.[44]

Given the spin-wave spectrum, the appropriate contribution to the low-temperature specific heat is readily computed. The internal energy of the spin-wave system is given by

$$\langle E\rangle = \textstyle\sum_k \epsilon_k^s n_k,\ k = 0,\ \pm 2\pi/L,\ \pm 4\pi/L,\ \pm\cdots, \tag{33}$$

where ϵ_k^s is the spin-wave dispersion relation defined (for small k) in Eq. (32), and the Bose factor n_k is

$$n_k = (e^{\epsilon_k^s/k_BT} - 1)^{-1}\ . \tag{34}$$

Converting the sum to an integral

$$\langle E\rangle = \frac{L}{2\pi}\int_{-\pi/a}^{\pi/a} \hbar V_s k (e^{\hbar V_s k/k_BT} - 1)^{-1}\,dk$$

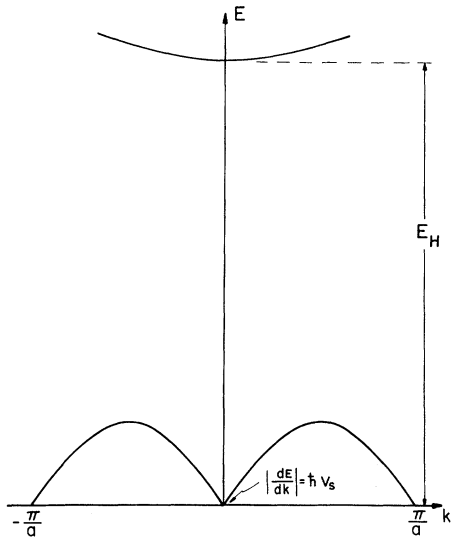

FIG. 11. Spin-wave dispersion relation and single-particle excitation band for the one-dimensional Hubbard model (see Ref. 16). The curves are drawn approximately to scale for NMP-TCNQ where E_H is approximately 0.1 eV at low temperature.

$$= 4\frac{L}{2\pi}\frac{(k_BT)^2}{\hbar V_s}\int_0^{x_M}\frac{x\,dx}{e^x-1} \quad , \tag{35}$$

where

$$x_M = \hbar V_s \pi / a k_B T \quad . \tag{36}$$

The factor of 4 in Eq. (35) arises from the $\pm k$ symmetry (a factor of 2) and the symmetry about $k = \pi/2a$ arising from the doubled unit cell of the AF ground state (a factor of 2). At low temperatures the integral in Eq. (35) is dominated at large k by the exponential so that negligible error is involved taking the limit of $x_M \to \infty$. The result, then, is

$$\langle E \rangle = \frac{2L}{\pi}\frac{(k_BT)^2}{\hbar V_s}\,\zeta(2) \quad , \tag{37}$$

where $\zeta(2) = \frac{1}{6}\pi^2$. Using $L = Na$, the specific-heat contribution is found to have the expected form

$$C = \alpha_M T = 6.58\, k_B^2 \frac{Na}{\pi\hbar V_s}\, T \quad . \tag{38}$$

Combining Eqs. (38) and (30) for $\chi(0)$ we obtain the result

$$\left.\frac{\alpha_M}{\chi(0)}\right|_{\text{theory}} = 3.29\left(\frac{k_B}{\mu_B}\right)^2 \quad . \tag{39}$$

There are two theoretical ambiguities involved in the specific-heat calculation, both having to do with the detailed nature of the spin-wave spectrum. First, Eq. (38) assumes each spin wave contributes with unit amplitude, i.e., the spectral weight associated with each mode integrates to unity. This is surely the case in the Heisenberg limit as $U_F/t \to \infty$ (except for the possibility of spin-wave interactions and of multiple spin-wave bound states; see below), but it is by no means obvious as U_F/t decreases. In fact, Takahashi[18] shows the persistance of the spin-wave spectrum to the limit $U_F = 0$, where one knows there is no spin-wave contribution. The suggestion, therefore, is that the spectral weight uniformly decreases as U_F/t decreases. A detailed Green's-function theory is required before this can be quantitatively cleared up. Fortunately, however, the analysis given below yields $U_F/t \sim 8$, so that the correction, if any, should be small. Such a correction would tend to decrease the theoretical value for $\alpha_M/\chi(0)$ given above. The second question involves spin-wave interactions and the possibility of multiple spin-wave bound states. Ovchinnikov in fact calculates the two spin-wave bound-state spectrum, and multiple spin-wave bound states will certainly exist in one dimension. This is intimately connected with the well-known fact that long-range order cannot exist in one dimension.[48] In spite of this it is known experimentally that the simple spin-wave theory provides a good description of the elementary excitations in one dimension. Again, it would appear that this is a question of the spectral weight. If the multiple spin-wave bound states contribute, they must "steal" spectral weight from the one spin-wave band. This shifting of spectral weight would tend to cancel in over-all effect on the thermodynamic properties. Again, a quantitative treatment would require a Green's-function theory. Our feeling, based on the above arguments, is that little error is involved in Eq. (39). Some quantitative insight into the accuracy of the theoretical result may be gained by considering the situation in the case of the Heisenberg model. Since the spin-wave result given in Eq. (39) is independent of the parameters U_F and t, and since the Heisenberg model is identical to the Hubbard model in the limit as $U_F/t \to \infty$, the Heisenberg results are relevant. In this case one has the numerical results of Bonner and Fisher[53] for the specific-heat and Griffiths's expression[61] for the zero-temperature susceptibility. Their ratio is

$$\left.\frac{\alpha_M}{\chi(0)}\right|_{\substack{\text{Heisenberg}\\ \text{theory}}} = 1.73\left(\frac{k_B}{\mu_B}\right)^2 \quad . \tag{40}$$

The experimental results presented above indicate that the strong-coupling limit is inappropriate for NMP-TCNQ. Nevertheless the Bonner-Fisher-Griffiths calculations suggest a limit for the error involved in Eq. (39). The exact result should be within the well-defined limits

$$1.73\left(\frac{k_B}{\mu_B}\right)^2 < \left.\frac{\alpha_M}{\chi(0)}\right|_{\text{theory}} < 3.29\left(\frac{k_B}{\mu_B}\right)^2 \quad . \tag{41}$$

Given the present status of the theory it is not possible to determine the theoretical ratio with better accuracy.

The theoretical prediction given in Eq. (41) may be compared with experiment by utilizing the measured specific-heat coefficient and the (extrapolated) zero-temperature susceptibility. The experimental ratio is evaluated as

$$\left.\frac{\alpha_M}{\chi(0)}\right|_{\text{expt}} = (2.6 \pm 0.3)\left(\frac{k_B}{\mu_B}\right)^2 \quad . \tag{42}$$

The numerical agreement *plus* the over-all qualitative features of the susceptibility and conductivity data combine to provide strong evidence of the applicability of the idealized one-dimensional Hubbard model to the NMP-TCNQ system.

The consistency of $\chi(0)$ and α_M with the model provides us with a numerical curve relating U_F and t for NMP-TCNQ. Equation (30) can be put in the form

$$\chi(0)\pi t/\mu_B^2 = I_0(x)/I_1(x) \quad , \tag{43}$$

where, again, $x = 2\pi t/U_F$. A second and independent relation is obtained from Ovchinnikov's expression for the single-particle energy gap as given in Eq. (28). This can be manipulated into the following form:

$$\frac{\chi(0)\pi t}{\mu_B^2} = \tfrac{1}{8}\pi^2 \frac{\chi(0)}{\mu_B^2} E_H [xf(x)]^{-1} , \tag{44}$$

where

$$f(x) = \int_1^\infty \frac{(y^2-1)^{1/2}dy}{\sinh xy} . \tag{45}$$

Regarding Eqs. 43 and 44 as two independent equations for the left-hand side as a function of x, we seek the value of x which gives a simultaneous solution. In computing the right-hand side of Eq. (44), the experimental values for $\chi_{(0)} = 2.2\times10^{-27}$ per molecule and $E_H = 0.1$ eV were inserted. The former is the extrapolated zero-temperature susceptibility value obtained directly from Fig. 6. The value utilized for the Hubbard gap is obtained from analysis of the low-temperature conductivity data of Shchegolev *et al.*[45] The data approach a straight line below 100 °K when plotted as $\ln\sigma$ vs $1/T$ with a slope corresponding to $0.035 \leq \frac{1}{2}E_H \leq 0.06$ eV (see Fig. 7). At the lowest temperatures the data curve away from the straight line; however, it seems likely that this is due to a small residual impurity induced conductivity. We shall assume the 0.05-eV value although a more direct measurement of E_H would be desirable. Evaluating the Hubbard gap from the conductivity involves the assumption that the exponential prefactor (essentially the carrier mobility) is only weakly temperature dependent. This is experimentally verified above 200 °K in the metallic phase; but has not been independently checked below 200 °K. If a better value of E_H becomes available, the results are readily corrected, for the value of the gap appears solely as a multiplicative constant on the right-hand side of Eq. (44).

The two relations [Eqs. (43) and (44)] are shown numerically in Fig. 12. The solution occurs at

$$x_0 = 2\pi t/U_F = 0.78 . \tag{46}$$

Inserting this value into Eq. (30), we obtain, for NMP-TCNQ,

$$U_F = 0.17\,\text{eV}, \quad t = 2.1\times10^{-2}\,\text{eV} . \tag{47}$$

The accuracy of these values (aside from the over-all question of the validity of the model) is limited to about 20% because of uncertainty in the correct value of the Hubbard gap as obtained from the conductivity data. Examination of Fig. 12 shows that because of the steepness of the numerical curves, the resulting values of U_F and t are relatively insensitive to small changes in E_H. The values quoted in Eq. (47) are quite reasonable in view of the discussion included in Sec. III.

The full bandwidth of $W = 4T \simeq 0.085$ eV is not surprising for a molecular crystal.[62-64] The very small value of U_F arises from a combination of the two effects discussed above; U_F involves the difference between U_0 and U_1, and each of those is considerably reduced from the corresponding bare values by cation (NMP) polarizability. Since estimates of the bare value of $(U_0 - U_1)$ fall in the range 0.5–1.0 eV and optical-absorption studies on KTCNQ give a value of 0.9 eV, the cation polarizability effect for NMP-TCNQ evidently amounts to a reduction by a factor of order 5. Thus the cation polarizability plays a crucial role in obtaining organic metals. Continued systematic work in this area with other cations will be quite valuable.

VII. TEMPERATURE DEPENDENCE

The magnetic susceptibility in the high-temperature metallic phase was identified above as the Pauli susceptibility, possibly enhanced by interaction effects. To analyze this in detail requires knowledge of the band structure of the electronic system in absence of interactions [see, for example, the bare susceptibility and RPA results of Eqs. (16) and (17)]. Within the tight-binding model this is easily obtained; the one-electron energy-band dispersion relation is given by

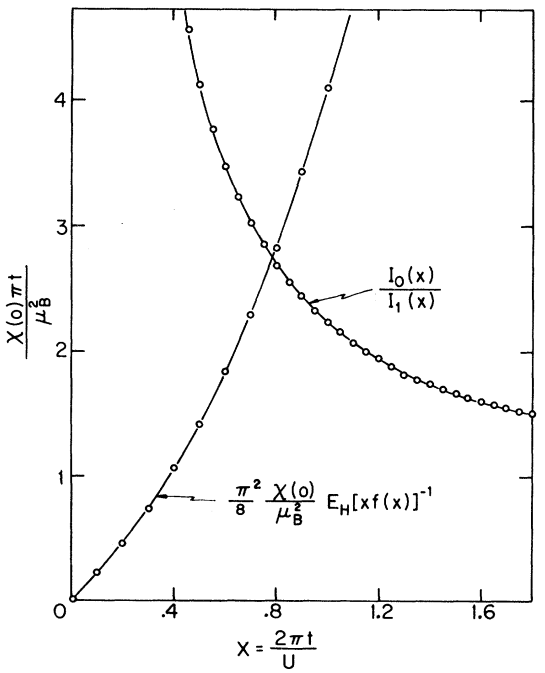

FIG. 12. Numerical solution of the coupled equations [(43) and (44)] for determination of U_F and t for NMP-TCNQ. The crossover occurs at $U_F/t \simeq 8$.

$$\epsilon(k) = -2t\cos ka\ , \tag{48}$$

from which the density of states per unit energy can be calculated:

$$2\rho(\epsilon)\,d\epsilon = (2N/\pi)(4t^2 - \epsilon^2)^{-1/2}\,d\epsilon\ . \tag{49}$$

The energy is measured relative to the center of the band. The above expression is the full density of states including the factor of 2 for spin [$\rho(\epsilon)$ is for one kind of spin only]. The Fermi energy E_F, when measured relative to the bottom of the band, is equal to twice the transfer integral for the case of one electron per molecule.

Using the value for $t = 2.1\times10^{-2}$ eV obtained from the low-temperature numerical analysis of the Hubbard model, one can estimate the bare Pauli susceptibility

$$(\chi_p)_{\text{theory}} = \mu_B^2/\pi t = 8.1\times10^{-28} \text{ per molecule.} \tag{50}$$

This is to be compared with the measured value 6.2×10^{-28} above 200 °K. The agreement is quite good. The point of particular interest is the obvious discrepancy with the RPA result of Eq. (17). In fact, using the low-temperature values of U_F and t, the RPA result is divergent predicting metallic ferromagnetism! The source of difficulty is clear; the RPA expression assumes that the Coulomb interaction can be treated in a Hartree or average way whereas the true situation involves strong Coulomb correlations which tend to keep the electrons apart. Theoretical attempts at building such correlations into the metallic state have been moderately successful.[10,65] The physics involved is the creation of a Coulomb "hole" around a given electron; the electron wave functions must be correlated to stay apart. Kanamori[66] has shown that under certain approximations the RPA result can be generalized to a form

$$\chi = 2\mu_B^2\,\frac{\rho}{1 - U_c\rho}\ , \tag{51}$$

where the correlated Coulomb interaction U_c is given by

$$U_c = \frac{U_F}{1 + U_F G_0} \ll U_F \tag{52}$$

and G_0 is a factor of order the reciprocal of the bandwidth. Detailed numbers are perhaps not important here; the important point is that correlations in the metallic state reduce the effective Coulomb interaction to a value much less than the bare value which dominates the low-temperature properties. This correlation can never reduce U_c all the way to zero, but the resulting actual enhancement factor for the susceptibility can be of order unity. We note that the measured value of 6.2×10^{-28} is actually *less* than the bare Pauli value 8.1×10^{-28} obtained from t. This difference is probably not significant and points not surprisingly to some limitation on the literal validity of the model. There is, however, the interesting possibility that the small experimental value is correct and is a manifestation of the reduced density of states near the Fermi surface predicted by Hubbard and Mott[67] as a precursor of the formation of the energy gap. A more direct measurement is needed as confirmation.

We conclude that Coulomb correlations in the metallic phase reduce the effective interaction essentially to zero leaving little or no enhancement to the susceptibility. On the other hand, as discussed in Sec. VI, the existence of a constant p_{eff} at least up to approximately 180–190 °K implies a rather sharp temperature variation of the effective correlated Coulomb interaction; the effective interaction remains large and temperature independent up to roughly 180 °K and then correlations take it rapidly toward zero. The correlation "hole" effect which seems to be so effective in the metallic state plays essentially no role at low temperature, for the system is condensed into an insulating phase where the electrons in the vicinity of an excitation cannot move out of the way without paying an energy at least equal to the single-particle gap E_H.

Note added in proof. In the atomic limit ($t/u \to 0$) all correlation arguments for reducing $U(t)$ are invalid, for an electron cannot "get out of the way" when another hops onto a given site [T. A. Kaplan and P. N. Argyres, Phys. Rev. B 1, 2457 (1970)]. On the other hand, for finite t, correlation is possible. Detailed theoretical studies are required to decide if it is possible, for $u/t \sim 8$ within the Hubbard model, to have sufficient correlation to explain the experiments.

In contrast to the variation of the effective Coulomb interaction with increasing temperature, the single-particle energy gap $E_H(T)$ appears to fall off more rapidly as can be seen simply from the conductivity data. The plots of σ vs T and ln σ vs T^{-1} indicate deviations from exponential behavior with fixed activation energy at 100 °K or below whereas the constant p_{eff} implies constant U_F below 180 °K. We conclude therefore that at relatively low temperatures either the gap begins to renormalize toward zero or, alternatively, conducting states begin to appear in the gap possibly because of fluctuations. More direct measurements of the temperature dependence of the gap are needed.

The picture presented for the metallic state is thus essentially that of the Landau-Fermi liquid[68] where the electron-electron Coulomb repulsion has little effect. The noninteracting low-energy quasiparticles give the system free-electron properties. For example, the magnetic susceptibility and electrical conductivity behave simply indicative of a

noninteracting electron system with a weakly temperature-dependent scattering time. The thermoelectric power (TEP) appears to be similarly simple above 200 °K. Figure 7 shows a negative TEP increasing in magnitude with increasing temperature. Such behavior is expected for a metallic system where the electronic contribution to the TEP is given by[69,70]

$$S = \frac{\pi^2 k_B^2}{3e} T \frac{\partial \ln\sigma}{\partial \epsilon}\bigg|_{\epsilon=0} , \tag{53}$$

where σ is the conductivity considered as a function of energy. The fact that S does not extrapolate to zero at $T=0$ in Fig. 7 implies the existence of an additional positive contribution. Equation (53) may be evaluated assuming the scattering time τ is not strongly energy dependent:

$$S = \frac{\pi^2 k_B^2}{3e} T \frac{\partial n(\epsilon)}{\partial \epsilon} \frac{1}{n(\epsilon)}\bigg|_{\epsilon=0}$$

$$\equiv \int_0^T \frac{C_e}{enT}\, dT, \tag{54}$$

$$S = \frac{2\pi k_B^2}{3eE_F} T , \tag{55}$$

where C_e is the electronic contribution to the specific heat. Equation (55) is obtained by assuming the one-dimensional density of states given in Eq. (47) taking into account both signs of spin. Again taking a Fermi-liquid point of view, the effect of electron-electron interactions would be a small mass enhancement in the electronic specific heat. Thus Eq. (54) can be applied directly. From the experimental slope above 200 °K, $\partial S/\partial T = 0.17\,\mu V/°K^2$, one obtains $\frac{1}{2}E_F = t = 0.046$ eV. The result is of the same magnitude (differing by only a factor of 2) as that obtained from the low-temperature analysis and the Pauli susceptibility. Again the analysis of the TEP must be considered only a crude first guess, a detailed transport theory not being available. Nevertheless, the agreement in the magnitude of the transfer integral gives the argument some credibility. Below 200 °K, a change in slope is observed and the electronic contribution appears to sharply decrease. This seems directly related to the transition to the magnetic insulating phase. It is clear that experimental studies of other transport properties, e.g., thermal conductivity,[71] together with related theoretical work would be valuable.

The ground state of the experimental NMP-TCNQ system is that of a magnetic insulator. The transition to the metallic phase is governed by the free energy $[F = U(T) - TS(T)]$ and therefore is driven by the entropy. Fundamentally, it is the entropy which thermodynamically forces the creation of electron-hole excitations. When the excitation

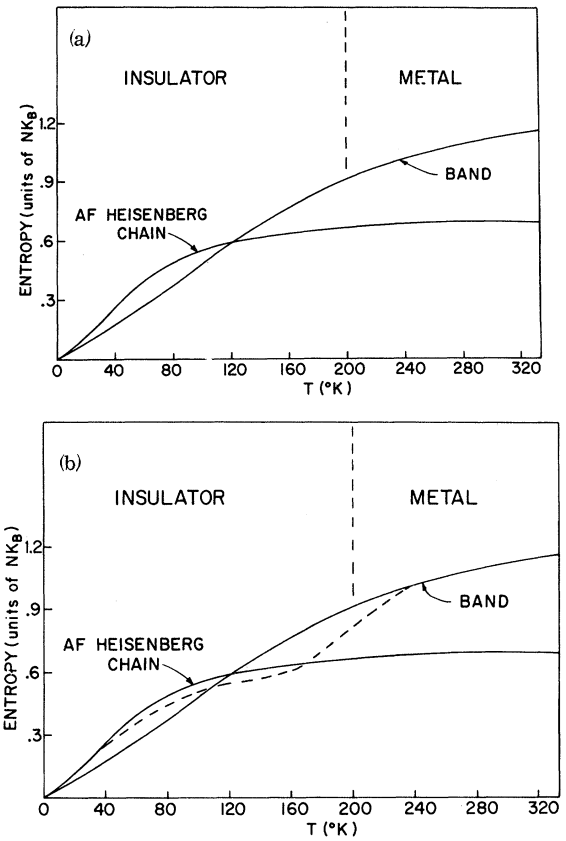

FIG. 13. (a) Computed entropy as a function of temperature for the linear Heisenberg AF chain (after Bonner and Fisher, Ref. 53) and the one-dimensional tight-binding metal. The curves were computed using values appropriate to NMP-TCNQ, $J = 2t^2/U_F = 5.2\times10^{-3}$ eV for the AF chain and $t = 2.1\times10^{-2}$ eV for the band entropy. (b) the curves of 13(a) are redrawn. In addition the approximate form of the true entropy for NMP-TCNQ is sketched.

density gets high enough for the formation of a significant Coulomb "hole," U_F correlates toward zero, and the metallic phase results. There are three contributions to the entropy:

(i) In the low-temperature insulating phase, when the spins begin to disorder, the entropy increases toward a value of order k_B ln2 per molecule (the exact value is unclear for this is not truly a spin-$\frac{1}{2}$ system). An idea of the functional dependence of the entropy on temperature can be obtained by going to the strong-coupling limit and examining the entropy for the Heisenberg model. The results of Bonner and Fisher for the one-dimensional Heisenberg infinite chain assuming $J = 2t^2/U_F = 5.2\times10^{-3}$ eV are shown in Fig. 13(a). The initial linear dependence is characteristic of the one-dimensional problem. Although the Heisenberg results are not directly appropriate to the NMP-TCNQ system, they should represent a reasonable approximation at low temperatures since experimentally $U_F/t \sim 8$.

(ii) At intermediate temperatures where the spin system is highly disordered each single-particle excitation removes of order $2k_B \ln 2$ while creating some free-carrier entropy (each excitation destroys *two* local moments at low temperature). Thus in this intermediate temperature regime we expect the actual NMP-TCNQ entropy to fall somewhat below the Heisenberg results.

(iii) In the metallic phase the entropy is given by

$$S = -k_B \sum_k [f_k \ln f_k + (1-f_k)\ln(1-f_k)] , \qquad (56)$$

where the sum is over all single-particle states (including spin). Using $f_k = (1+e^{\epsilon(k)/k_B T^{-1}}$ and the one-electron dispersion relation for the tight-binding energy band [Eq. (48)] one obtains

$$S = 2\frac{Nk_B}{\pi}\int_0^{\pi}\left(\frac{\ln(e^{-D\cos x}+1)}{e^{-D\cos x}+1} + \frac{\ln(e^{D\cos x}+1)}{e^{D\cos x}+1}\right) dx, \qquad (57)$$

where $D = 2t/k_B T$ and N is the number of electrons. Assuming $t = 2.1\times 10^{-2}$ eV and performing the numerical integration, one obtains the computed band entropy curve shown in Fig. 13. At high temperatures the entropy asymptotically approaches $Nk_B \ln 4$. This limit follows from the finite bandwidth and is easily understood. When the temperature exceeds the Fermi temperature each of the N k states is accessible and for each there are four possibilities: singly occupied with spin up, singly occupied with spin down, doubly occupied, and unoccupied. Since each of these has equal weight, the resulting entropy is $k_B \ln 4$.

Figure 13(a) gives a reasonably clear picture of the physical situation. At low temperatures the antiferromagnetic disorder favors the insulating state, whereas above roughly 150 °K the metallic state would have the higher entropy. Evidently the system evolves continuously from one limit toward the other with corrections due to the single-particle excitations in the insulator as discussed above. Since the existence of a gap must decrease the band entropy and since the existence of these excitations decreases the disordered localized moment contribution, the true entropy curve might have a temperature dependence roughly as the dotted line in Fig. 13(b). This dotted curve in Fig. 13(b) is a sketch based on the above arguments and the computed curves of Fig. 13(a). It is of interest to note that, if the M-I transition temperature is comparable with the Fermi temperature, Fig. 13 (b) suggests a diffuse and gradual transition. In fact, since in one dimension the ground state is insulating for any finite U_F, and since the entropy curves in Fig. 13(a) cross only once, the M-I transition in a one-dimensional system must occur at a relatively high temperature and must be very smooth. The situation for a three-dimensional system is fundamentally different, for the low-temperature AF spin disorder entropy varies as T^3 [rather than T as in Figs. 13(a) and 13(b)]. As a result, in three dimensions the band entropy is greater than that of the AF insulator for a sizable range of temperatures *less than the Néel temperature*. In this case the curves would cross twice so that there would be two temperature regions where the entropy favors a transition to the metallic state. Again if the M-I transition temperature is comparable with the Fermi temperature, the transition will be gradual. However, if the energetics are such that a transition could occur below the AF transition temperature (i.e., if the ground-state energies are sufficient close) one can see a tendency toward a first-order transition driven by the increased band entropy relative to that of the ordered AF state. The latter alternative is reminiscent of the experimental situation in such systems as V_2O_3.[7]

It seems evident from Fig. 13(b) that no large specific-heat anomaly is to be expected at the metal-insulator transition or in the region of AF disorder in NMP-TCNQ. In both cases the breadth of the one-dimensional transition together with the large molecular background specific heat makes it unlikely that any anomaly would be observable. The theory for the one-dimensional Heisenberg AF[54] predicts no sharp peak at any temperature, and attemps to observe the magnetic contribution in other systems have failed.[72] Estimates for spin $\frac{1}{2}$ indicate a broad specific-heat maximum of less than 1 cal mole^{-1} deg^{-1} which would be difficult to separate from the lattice contributions which dominate in the range 30–60 °K. The full experimental specific-heat curve is shown as a function of temperature in Fig. 14. The heat capacity is clearly dominated by molecular bending and rotational modes as well as lattice phonons at all but the lowest temperatures.

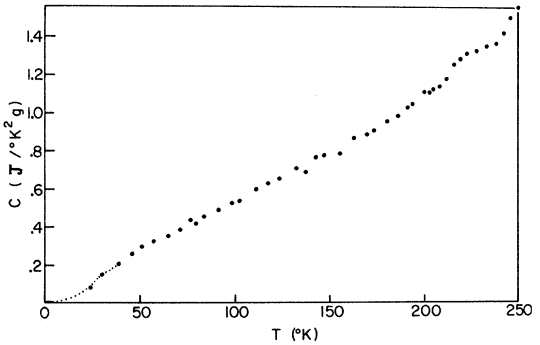

FIG. 14. Specific heat per gram of NMP-TCNQ as a function of temperature. For details of the low-temperature behavior see Fig. 8.

VIII. SPIN-RESONANCE STUDIES

Because of the relatively small spin-orbit constants associated with the first-row elements (C, N, H) from which the molecules of NMP-TCNQ are synthesized, the coupling of the spins to the lattice is extremely weak. This fact has made it possible to use the spin resonance as a means to measure the susceptibility in the metallic phase, through the metal-insulator transition and into the insulating regime (both AF and paramagnetic).

High-field spin-resonance studies on single crystals (at X band and Q band) showed a narrow line with g value extremely close to the free-electron value. The anisotropy in g was of order

$$|g_\perp - g_\parallel|/g \simeq 4\times 10^{-4} \quad , \tag{58}$$

and the deviation from the free-electron value was of the same magnitude. A g shift of this magnitude is quite reasonable. One expects $\Delta g/g \sim \lambda/\Delta E$, where λ is the spin-orbit coupling constant and ΔE is the energy separation to the next band. The strong visible absorption of the $TCNQ^-$ radical implies a value for $\Delta E \sim 2$eV. Thus the measured $(\Delta g/g)$ requires a value for λ of order 8×10^{-4} eV in good agreement with the known magnitude of the spin-orbit interaction for carbon and nitrogen.

Detailed linewidth measurements as a function of temperature were carried out at 30 MHz (approximately 10-G external magnetic field) on powder samples. The advantages of the low-frequency powder measurement are threefold. First, the very low field makes small g-value anisotropy completely unimportant, so that the measured linewidth is intrinsic. Second, the low frequency eliminates any possible skin depth problem associated with resonance in the metallic state. Third, our chemical synthesis techniques provided maximum purity on the powder samples. The linewidth results are shown in Fig. 15. Throughout the entire temperature range the line remains unshifted (a shift of a fraction of a gauss would easily be detected).

The existence of an unshifted narrow resonance in the antiferromagnetic phase is of particular interest. Although the argument given above concerning the small spin-orbit interaction is correct, conventional theory (either semiclassical or spin-wave analysis) based on the *Néel model of the AF state* yields the well-known result that in zero field the AF resonance occurs at[73]

$$\omega_0^{AF} = \gamma(2H_E H_A)^{1/2} \, , \tag{59}$$

where H_E and H_A are the exchange and anisotropy fields, respectively. One can estimate H_E from the measured values of t and U_F for

$$J \sim \mu_B H_E \simeq 2t^2/U_F \simeq k_B T_N \quad , \tag{60}$$

giving $H_E \simeq 10^6$ G. Thus the above simple expression would predict a shift of order $10^3 H_A^{1/2}$ indicating that anisotropy fields as small as 10^{-6} G would have a large effect. This is not observed experimentally.

The error in the above argument is that it is founded on a small-deviation spin-wave theory based on the Néel model of the AF state. Although such a picture gives an excellent description for large spin in three dimensions where the coordination number is large, it is grossly misleading for the highly quantum-mechanical spin-$\frac{1}{2}$ AF in one dimension. In the latter case, the correlation time for a particular Néel configuration is evidently extremely short, of order $\hbar/J$. It is for this reason that the AF zero-point deviation diverges in one dimension[49] whereas in a typical three-dimensional case the zero-point deviation amounts to a few percent correction to the sublattice magnetization.[49] The short correlation time in one-dimensional spin-$\frac{1}{2}$ case is to be contrasted with Anderson's estimate[74] of several years for the lifetime of a typical Néel configuration in a three-dimensional system.

The detailed spin-resonance dynamics have not been worked out for the one-dimensional antiferromagnet including anisotropy and dipolar effects. Ovchinnikov's spin-wave specturm[16] goes to zero energy as $k \to 0$, π implying the existence of the usual two AF resonance modes. However, we expect the low-spin one-dimensional case to be insensitive of anisotropy effects. The essential question is whether or not a particular Néel-like configuration persists long enough for the system to precess in, and thereby sense, the anisotropy or dipolar field. The relevant comparison has its origin in the uncertainty principle and is between τ_c and $(\omega_0^{AF})^{-1}$. If τ_c is much less than $(\omega_0^{AF})^{-1}$ the anisotropy effects are essentially motionally narrowed out of the picture. We therefore suggest that the unshifted narrow resonance in the AF phase provides considerable insight into the nature of the one-dimensional antiferromagnet. The correlation time is evidently very short, suggesting a picture of resonating singlets.

Evidence for a short correlation time can be obtained directly from the linewidth data of Fig. 15. For reference, the temperature regions corresponding to insulating AF, insulating paramagnet, and metal are indicated on the figure. The overall shape suggest two mechanisms. At high temperatures a contribution linear in T appears to dominate. Below the M-I transition the linewidth goes through a broad maximum with decreasing temperature, the maximum occuring roughly at the temperature where the AF spin correlations become important. As anticipated the narrow Lorentizian lines

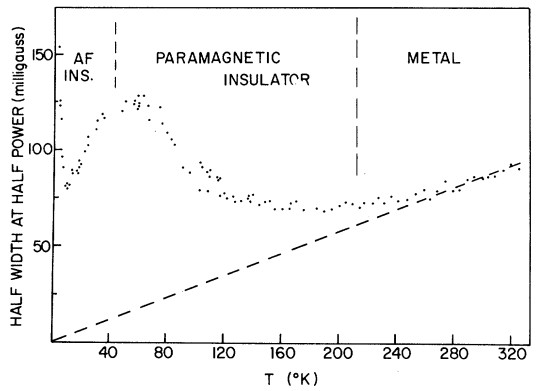

FIG. 15. Half-width at half-amplitude of the ESR absorption curves for NMP-TCNQ in milligauss vs temperature. Since the line shape was Lorentzian, the half-width at half-amplitude ($\frac{1}{2}\Delta H_{1/2}$) is related to the measured peak-to-peak linewidth of the derivative curve (ΔH_{pp}) by $(\frac{1}{2}\Delta H_{1/2})/(\Delta H_{pp}) = \frac{1}{2}\sqrt{3}$.

indicate motional narrowing of the dipolar linewidth.[75,76] In the insulating phase, such motional narrowing is expected as a result of the exchange interaction between sites which gives rise at low temperatures to the antiferromagnetism ($\tau_c \simeq \omega_{ex}^{-1}$). In the metallic phase the electrons move more or less freely through the crystal in the tight-binding energy band; the resulting correlation time should be of order $\tau_c = a/v_F$, where a is the lattice constant and v_F is the Fermi velocity, $v_F = \hbar^{-1} d\epsilon_k/dk|_0$. Thus we expect

$$\tau_c = \omega_{ex}^{-1} = \hbar/J \simeq 10^{-13} \text{ sec}, \quad \text{paramagnetic insulator}$$
$$\frac{a}{v_F} = \frac{a\hbar}{d\epsilon_k/dk|_0} = \frac{\hbar}{2t} = 10^{-14} \text{ sec}, \quad \text{metal.} \tag{61}$$

Naturally, since the system evolves continuously from metal to insulator, the correlation time will vary continuously as well. The dipolar contribution to the second moment of the resonance line can be estimated from the Van Vleck formula[77] using the crystal structure of NMP-TCNQ,[32] and the molecular spin density distribution of Lowitz,[29] and the reduced moment found in the insulating phase. The resulting value (including the $\frac{10}{3}$ factor) of $\langle \Delta\omega_D^2 \rangle = 2.7 \times 10^{-19}$ sec^{-2} can be used to obtain τ_c directly from experiment with the relation

$$\Delta\omega_{expt} = \langle \Delta\omega_D^2 \rangle \tau_c \quad . \tag{62}$$

The resultant τ_c should reflect the correct temperature dependence although the precise value is scaled to the estimated dipolar contribution. $\Delta\omega_{expt}$ is obtained from the data of Fig. 16 by subtracting off the underlying linear term and attributing the difference to Eq. (62). This assumes the linear term arises from spin-lattice relaxation and that this contribution persists to low temperatures; however, the effect of this assumption on the resulting low temperature τ_c is minimal so long as *this contribution* to T_1 decreases uniformly with decreasing temperature. Since as shown below the linear term arises from the coupling of the spins to phonons and molecular vibrations, this should be the case.

The experimentally determined τ_c is shown as a function of temperature in Fig. 16. One sees a value of the expected magnitude in the metallic state. As the temperature decreases τ_c increases smoothly reaching a maximum of 7.5×10^{-14} sec at 50 °K. On decreasing the temperature further well into the AF regime τ_c *again decreases* apparently stabilizing at $\tau_c \simeq 5 \times 10^{-14}$ sec at the lowest temperatures. Thus the experimental linewidth studies indicate that the one-dimensional AF ground state is characterized by a correlation time $\tau_c \simeq \omega_{ex}^{-1}$ as argued above.

The maximum in τ_c corresponds to the slowing down of the fluctuations in the vicinity of the magnetic "transition." For a true phase transition in three dimension, τ_c slows down essentially to zero,[78] giving a divergence in the linewidth[79] (the full dipolar second moment becomes operative), and at lower temperatures the resonance is shifted according to Eq. (59). Because of the large fluctuations in the one-dimensional system,[80] τ_c remains relatively short throughout the broad transitional region. These experimental data provide a unique picture of the one-dimensional AF transition showing clearly both the large fluctuations as well as the broad transitional region.

The question of exchange narrowing in one-dimensional systems has recently received special attention in the literature.[81,82] Experimental studies on single crystals of TMMC have shown large anisotropies in linewidth and line shape. Such effect are not evident in our low-field powder data, although the over-all magnitude of the linewidth may be affected. However, averaging the TMMC data over all angles yields an estimated powder linewidth with magnitude in close agreement with the results of conventional exchange narrowing theory. Thus the use of Eq. (62) to obtain τ_c from the powder data should involve little error.

The linear temperature dependence of the linewidth which becomes evident in the metallic phase suggests a direct spin-phonon relaxation process where the rate is proportional to the number of thermal phonons. Such a process was first proposed by Overhauser,[83] and the mechanism was developed by Elliott[84] and Yafet.[85] Elliott argued that the spin-flip lifetimes τ_s should scale with the simple scattering lifetime τ_R, there being a finite probability of a spin flip whenever the electron is scattered. The dimensionless scaling parameter in Elliott's theory was the g shift which

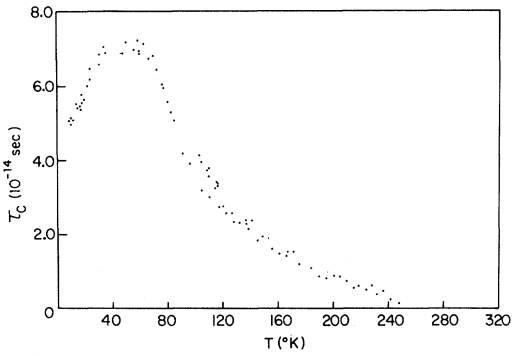

FIG. 16. Correlation time τ_c vs temperature for NMP-TCNQ as obtained from the linewidth data of Fig. 15.

is a measure of the strength of the spin-orbit interaction:

$$\tau_s^{-1} \simeq C(\Delta g/g)^2 \tau_R^{-1} \quad , \tag{63}$$

where C is a constant of order 10^{-1}. Since we know from the spin resonance that $(\Delta g/g)^2$ is of order 10^{-7}, τ_s can be estimated from the electrical conductivity in the metallic phase. Following Ziman,[86] the conductivity is calculated from the expression for the current density $\vec{J}$:

$$\vec{J} = 2\sum_k e^2 \tau_R \vec{v}_k (\vec{v}_k \cdot \vec{E}) \left(-\frac{\partial f^0}{\partial \epsilon}\right) , \tag{64}$$

where $\vec{E}$ is the applied field, $\vec{v}_k$ is the velocity for an electron in the state with wave vector $\vec{k}$, and f_0 is the Fermi distribution function. Using the one-dimensional tight-binding band structure given by Eq. (48) with the implied planar Fermi surface, the current density can be evaluated:

$$\vec{J} = \frac{2Ve^2}{(2\pi)^3} \int \vec{v}_k \left(-\frac{\partial f^0}{\partial \epsilon}\right) \tau_R (\vec{v}_k \cdot \vec{E}) d^3k \quad , \tag{65}$$

$$\vec{J} = \frac{2Ve^2}{(2\pi)^3} \int\int \vec{v}_k (\vec{v}_k \cdot \vec{E}) \left(-\frac{\partial f^0}{\partial \epsilon}\right) \tau_R \frac{dS}{(\hbar \vec{v}_k)} \, d\epsilon \ , \tag{66}$$

where dS is the differential area on the surface of constant energy at ϵ. Solving for J_x with $\vec{E} = E_x \hat{x}$ ($\hat{x}$ is taken as the unit vector in the direction of highest conductivity) we obtain

$$J_x = \frac{2V}{(2\pi)^3} \frac{e^2 \tau_R E_x}{\hbar} \int\int |v_{kx}| \left(-\frac{\partial f^0}{\partial \epsilon}\right) dS \, d\epsilon \tag{67}$$

$$= \frac{2V}{(2\pi)^3} \frac{e^2 \tau_R E_x}{\hbar} \int |v_{kx}| \, dS_F \tag{68}$$

$$= \frac{2V}{(2\pi)^3} \frac{e^2 \tau_R E_x}{\hbar} v_F \left[2\left(\frac{2\pi}{b}\right)\left(\frac{2\pi}{c}\right)\right] , \tag{69}$$

and $2\pi/b$ and $2\pi/c$ are lattice constants. The integral in Eq. (68) is restricted to the first Brillouin zone. The result therefore is

$$J_x = \frac{2Na}{\pi\hbar} \, e^2 \tau_R v_F E_x \ , \tag{70}$$

so that the conductivity is given by

$$\sigma_{xx} = \frac{J_x}{E_x} = \frac{N e^2 \tau_R v_F^2}{\pi t} \ . \tag{71}$$

Substituting the Fermi velocity from Eq. (61), one finds

$$\sigma_{xx} = \frac{4N}{\pi} \frac{e^2 \tau_R}{\hbar^2} \, ta^2 \ . \tag{72}$$

From the measured value of σ at room temperature one can estimate $\tau_R \sim 10^{-14}$ sec. Using this together with the value for $\Delta g/g$, we estimate $\Delta\omega = \tau_s^{-1} \sim 10^6$ in agreement with experiment. Thus the order of magnitude is correct, and the linear temperature dependence is consistent with the observed decrease in conductivity with increasing temperature in the metallic phase. The microscopic treatment of this relaxation mechanism has been developed by Yafet.[85] Using Yafet's theory, one finds[87] that in order to obtain a relaxation rate in agreement with experiment requires a spin-flip matrix element via the spin-orbit interaction which is roughly one-third of the corresponding value for sodium metal; this is a reasonable value, since C and N are expected to have spin-orbit coupling somewhat smaller than Na. Clearly, as in any relaxation or linewidth study, other mechanisms for a linewidth linear in T are possible. However, the order-of-magnitude numerical agreement described above suggests that the process is correctly indentified.

IX. SUMMARY AND CONCLUSION

The experimental studies and analysis presented in this paper give a detailed picture of the metal-insulator transition and the associated evolution of a single system from metal to paramagnetic insulator to antiferromagnetic insulator as the temperature is lowered.

Comparison of the low-temperature experimental results with the predictions of exact solutions of the one-dimensional Hubbard Hamiltonian imply that NMP-TCNQ is a nearly ideal example of this important and much studied model. The temperature dependences of the experimental parameters are in qualitative agreement with expectations. However, the need for a satisfactory finite-temperature theory is all too evident. Of particular importance is a sound treatment of the build-up of electron-hole correlations toward the formation of the Coulomb "hole" responsible for the small effective electron-electron Coulomb repulsion in the metallic state.

The low-temperature one-dimensional antiferromagnetic state was studied by resonance and specific-heat techniques. The predicted linear term characteristic of one-dimension has been observed in the specific heat. The resonance studies, including the unshifted position of the spin-resonance line together with the observed temperature dependence of the linewidth have provided insight into the one-dimensional antiferromagnet. The fluctuations expected for a one-dimensional "phase transition" have been seen in the linewidth study. A slowing down of the fluctuations is observed in the transitional region; however, the correlation time never grows longer than roughly 10^{-13}sec. The implications of these studies on the general question of one-dimensional "phase transitions" are clear. The transitional regions are broad ($\Delta T \sim 20\,^{\circ}$K) both in the case of the M-I transition near 200 °K and the AF transition near 40 °K. Nevertheless, below the transitional temperature region the physical properties of the system are established; i. e., the system is definitely insulating with an energy gap below 100 °K, and the AF spin waves exist and are well defined below 10 °K. It would thus appear obvious that the theorem regarding the absence of long-range order in one dimension should not be used as an argument against the study of and search for interesting phenomena in one-dimensional systems.

The basic parameters relating to the molecular physics in the solid are the effective Coulomb interaction $U_{\text{eff}} \simeq 0.17$ eV and the intermolecular transfer interaction $t \simeq 2.1 \times 10^{-2}$ eV. The latter implies a metallic bandwidth of order 0.1 eV, a value which is reasonable for a molecular crystal. However, wide variations in the transfer integral can be expected to result from small changes in lattice structure and from small changes in the detailed π molecular wave functions in the particular structure of interest since the intermolecular overlap is extremely sensitive to such effects. A direct tight-binding band calculation in which t is evaluated from the SCFMO wave functions for $TCNQ^-$ in the lattice structure of NMP-TCNQ for comparison with the experimental value would be of considerable interest. The small value for U is somewhat more surprising. The basic mechanisms for reducing the effective Coulomb interaction are discussed in Secs. I and III. First, molecular correlation effects reduce the interaction from an atomic value (~ 10 eV) to an order of 2–3 eV. The importance of the molecular correlation cannot be overemphasized, for without this effect metallic organic systems would not be possible. Second, the bare interaction is reduced by a factor estimated to be of order 5 by the cation polarizability of the NMP molecules. The experimental evidence on this important point is quite convincing. The optical data on KTCNQ and on Cs_2TCNQ_3 show the charge-transfer excitation at about 1 eV. This band is definitely shifted to lower energies in the N-methyl-phenazinium salt. Resistivity studies are inconsistent with a low-temperature gap larger than about 0.1 eV. Diffuse reflectance studies show an absorption band at about 0.4 eV, [88] but the position of the band edge (which determines the gap) cannot be determined from the data, nor is it clear that this absorption corresponds to the production of current carrying excitations. In any case, there is no doubt that the effective Coulomb interaction is significantly reduced in the NMP salt as compared with the alkali salts. The bare on-site interaction, U_0 should be insensitive to the detailed surroundings. The nearest-neighbor interaction U_1 might well change with the detailed molecular arrangement in the crystal. However, it is unlikely that U_1 could increase by 20% on going from the alkali to the NMP salt, especially since the molecules are displaced from one another in NMP-TCNQ in such a way as to *decrease* the near-neighbor Coulomb interaction. Moreover, the general tendency toward better conductivity (and hence smaller band gaps) with polarizable organic cations has been clear for many years. [23] Thus, the experiments indicate a reduction of the difference $U_0 - U_1$ by the polarizability factor to the relatively small value of 0.17 eV for NMP-TCNQ. The cation polarizability evidently plays a key role in making the metallic state possible; without it, the basic Coulomb interaction would be in the range of 1 eV as compared with a bandwidth of 0.1 eV, and the metallic state would be out of reach.

The chain of $TCNQ^-$ molecules stacked face to face with surrounding chains of NMP is in a crude sense reminiscent of Little's suggested model for an organic superconductor. [39] From this point of view the NMP cations play the role of the side chains to the TCNQ "spine." Although the ideas originally put forward by Little have received considerable attention, [89] we believe the work described in this paper represents the first example of an experimental situation in which the cation polarizability can be shown to play a definitive role. Although we have not yet pursued this in depth, it seems evident that in the metallic state a mass enhancement of the electrons is implied as a result of virtual emission and reabsorption of polarization quanta (excitons) which at the same time provide an indirect attractive term to the electron-electron interaction. Whether the over-all interaction can ever be attractive with the proper frequency dependence to give super conductivity [90] is much less clear; although possible, it is perhaps not likely except under very stringent conditions. However, it is worth emphasizing once again that further reduction of the basic intramolecular Coulomb repulsion through correlation is quite pos-

sible.[91] It seems that the best procedure at present is to attempt to maintain the metallic state to lower temperatures.

In addition to the many aspects of the metal-insulator transition, the theoretical description of the transport properties in a narrow-band system at temperatures comparable to the Fermi temperature is a fascinating and challenging problem. The difficulty can be seen from an estimate of the mean free path $\Lambda \sim v_F \tau$, where v_F is the Fermi velocity and τ the scattering time. Using the values estimated in Sec. VIII, one obtains a value for Λ of roughly one lattice constant; the electrons in effect scatter at every site! This represents a breakdown of the adiabatic approximation as discussed by Ziman.[92] The essential difficulty can be anticipated by looking at the widths of optical-absorption lines corresponding to the π-π^* transition in aromatic systems[93] where a typical width of a few hundred cm^{-1} is found at room temperature. Since the electrons in question here propogate in a band arising from such a π^* level of TCNQ and since the resulting energy bandwidth is of the same magnitude, the difficulty is clear. At low temperatures, where the one-molecule levels would be sharp, a conventional theory is adequate, and τ could be calculated with perturbation theory. At higher temperatures, when $\tau E_F \sim \hbar$, the usual approximations break down. In this regime the situation is perhaps more properly viewed as that of electrons propagating in a band and simultaneously subjected to a random (in space *and* time) scattering potential of rms amplitude proportional to kT. The question of electrons propagating in a random potential has recently become of interest in connection with the problem of amorphous materials. There, where the potential is spatially random but *time independent*, Anderson's theory[94] predicts the formation of localized states. The random time dependence qualitatively changes the problem. In this case it seems that the electrons would continue to propagate, but in a hindered fashion depending critically on the time fluctuations in the local potential. This interesting problem requires further study before the conductivity in such narrow-band metals can be understood.

In this paper we have presented a detailed experimental study of the metal-insulator transition and related phenomena in the organic solid, NMP-TCNQ. This system is particularly interesting, for it is representative of a class of materials which heretofore have had little impact on the electronic aspects of solid-state physics namely, solids made up entirely of organic molecules consisting solely of carbon, nitrogen, and hydrogen. The possibility of designing and synthesizing molecules to achieve properties on the molecular scale that will lead to interesting and fundamental solid-state physics suggest an exciting future for this area of research.

ACKNOWLEDGMENTS

The authors wish to thank Professor P. Pincus for his help and continued interest, Professor J. R. Schrieffer for several stimulating discussions, Dr. J. Kimball for helping clear up some theoretical questions, P. Nigrey for careful sample preparation, and Professor R. Glover for asking a penetrating question. One of us (A. F. G.) wishes to acknowledge support from the Dupont Young Faculty Grant.

---

*Work partially supported by the National Science Foundation and is a contribution from the Laboratory for Research on the Structure of Matter (supported by ARPA).

†In partial fulfillment of requirements for the Ph. D. degree, University of Pennsylvania, 1971.

[1]N. F. Mott, Proc. Phys. Soc. (London) A62, 416 (1949).

[2]I. G. Austin and N. F. Mott, Science 168, 71 (1970), and other references cited therein.

[3]S. Doniach, Advan. Phys. 18, 819 (1969).

[4]W. A. Harrison, *Pseudopotentials in the Theory of Metals* (Benjamin, New York, 1966), Secs. 8–11, and references cited therein.

[5]W. Kohn, Phys. Rev. Letters 19, 439 (1967).

[6]D. Adler, in *Solid State Physics*, edited by F. Seitz, D. Turnbull, and H. Ehrenreich (Academic, New York, (1968), Vol. 21; see also Rev. Mod. Phys. 40, 673 (1968).

[7]D. B. McWhan and J. P. Remeika, Phys. Rev. B 2, 3734 (1970); A. Jayaraman, D. B. McWhan, J. P. Remeika, and P. D. Dernier, *ibid.* 2, 3751 (1970); A. Menth and J. P. Remeika, *ibid.* 2, 3756 (1970); A. C. Gossard, D. B. McWhan, and J. P. Remeika, *ibid.* 2, 3762 (1970); K. Andres, *ibid.* 2, 3768 (1970); P. D. Dernier and M. Marezio, *ibid.* 2, 3771 (1970).

[8]A. Menth, E. Buehler, and T. Geballe, Phys. Rev. Letters 22, 295 (1969).

[9]J. Hubbard, Proc. Roy. Soc. (London) A276, 238 (1963); A277, 237 (1963); A281, 401 (1964).

[10]C. Herring, in *Magnetism*, edited by G. T. Rado and H. Suhl (Academic, New York, 1968), Vol. IV.

[11]M. C. Gutzwiller, Phys. Rev. 137, A1765 (1965).

[12]M. Cyrot, Phys. Rev. Letters 25, 871 (1970).

[13]W. Langer, M. Plischke, and D. Mattis, Phys. Rev. Letters 23, 1448 (1969); D. C. Mattis and W. D. Langer, *ibid.* 25, 376 (1970).

[14]W. F. Brinkman and T. M. Rice, Phys. Rev. B 2, 4302 (1970).

[15]E. H. Lieb and F. Y. Wu, Phys. Rev. Letters 20, 1445 (1968).

[16]A. A. Ovchinnikov, Zh. Eksperim. i Teor. Fiz. 57, 2137 (1969) [Sov. Phys. JETP 30, 1160 (1970)].

[17]I. A. Musurkin and A. A. Ovchinnikov, Fiz. Tverd. Tela 12, 2524 (1970) [Sov. Phys. Solid State 12, 2031 (1970)].

[18]M. Takahashi, Progr. Theoret. Phys. (Kyoto) 43, 1619 (1970); 42, 1098 (1969); 43, 860(E) (1970).

[19]R. E. Peierls, *Quantum Theory of Solids* (Oxford U. P., London, 1955), p. 108.

[20]D. Adler and H. Brooks, Phys. Rev. 155, 826 (1967).

[21]J. C. Slater, Phys. Rev. 82, 538 (1951).

[22]R. Ramirez, L. M. Falicov, and J. C. Kimball, Phys. Rev. B 2, 3383 (1970).

[23]O. H. LeBlanc, Jr., in *Physics and Chemistry of the Organic Solid State*, edited by M. M. Labes, D. Fox, and A. Weissberger (Interscience, New York, 1967), p.133.

[24]P. L. Nordio, Z. G. Soos, and H. M. McConnell, Ann. Rev. Phys. Chem. 17, 237 (1966).

[25]R. G. Kepler, P. E. Bierstedt, and R. E. Merrifeld, Phys. Rev. Letters 5, 503 (1960); W. J. Siemons, P. E. Bierstedt, and R. G. Kepler, J. Chem. Phys. 39, 3523 (1963); R. G. Kepler, *ibid.* 39, 3528 (1963).

[26]R. W. Tsien, C. M. Huggins, and O. H. LeBlanc, Jr., J. Chem. Phys. 45, 4370 (1966).

[27]L. R. Melby, R. J. Harder, W. R. Hertler, W. Mahler, R. E. Benson, and W. E. Mochel, J. Am. Chem. Soc. 84, 3374 (1962).

[28]C. J. Fritchie, Jr., J. Chem. Soc. A 1328 (1969).

[29]D. A. Lowitz, J. Chem. Phys. 46, 4698 (1967).

[30]P. H. Rieger and G. K. Fraenkel, J. Chem. Phys. 37, 2795 (1962).

[31]R. E. Long, R. A. Sparks, and K. N. Trueblood, Acta Cryst. 18, 932 (1965).

[32]C. J. Fritchie, Jr., Acta Cryst. 20, 892 (1966).

[33]R. G. Parr, *Quantum Theory of Molecular Electronic Structure* (Benjamin, New York, 1964).

[34]J. C. Schug and M. Karplus, J. Chem. Phys. 37, 330 (1962).

[35]J. G. Vegter and J. Kommandeur, Proceedings of Conference on Molecular Crystals, Philadelphia, Pa., 1970 (unpublished).

[36]S. Hiroma, H. Kuroda, and H. Akamata, Bull. Chem. Soc. Japan 44, 9 (1971).

[37]O. H. LeBlanc, Jr., J. Chem. Phys. 42, 4307 (1965).

[38]C. G. LeFevre and R. J. LeFevre, Rev. Pure Appl. Chem. 5, 261 (1955).

[39]W. A. Little, Phys. Rev. 134, A1416 (1964).

[40]N. S. Hush and J. Blackledge, J. Chem. Phys. 23, 514 (1955); G. J. Hoijtink, Rec. Trav. Chim. 74, 1525 (1955); G. J. Hoijtink, E. DeBoer, and P. H. Van der Meij, *ibid.* 75, 487 (1956).

[41]R. M. Hedges and F. A. Matsen, J. Chem. Phys. 28, 950 (1958).

[42]L. R. Melby, Can. J. Chem. 43, 1448 (1965).

[43]R. T. Schumacher and C. P. Slichter, Phys. Rev. 101, 58 (1956).

[44]A. J. Epstein, S. Etemad, A. F. Garito, and A. J. Heeger, Solid State Commun. 9, 1803 (1971); A. J. Epstein, A. F. Garito, and A. J. Heeger, Bull. Am. Phys. Soc. 16, 636 (1971); S. Etemad, A. F. Gartio, and A. J. Heeger, *ibid.* 16, 636 (1971).

[45]I. F. Shchegolev, L. I. Buravov, A. V. Zvarykina, and R. B. Lyubovskii, Zh. Eksperim. i Teor. Fiz. Pis'ma v Redaktsiyu 8, 353 (1968) [Sov. Phys. JETP Letters 8, 218 (1968)].

[46]L. I. Buravov, D. N. Fedutin, and F. I. Shchegolev, Zh. Eksperim. i Teor. Fiz. 59, 1125 (1970) [Sov. Phys. JETP 32, 612 (1971)].

[47]P. A. Wolff, Phys. Rev. 120, 814 (1960).

[48]L. D. Landau and E. M. Lifshitz, *Statistical Physics* (Addison-Wesley, Reading, Mass., 1958), Sec. 149.

[49]R. Kubo, Phys. Rev. 87, 568 (1952).

[50]J. Van Kranendonk and J. H. Van Vleck, Rev. Mod. Phys. 30, 1 (1958).

[51]J. des Cloizeaux and J. J. Pearson, Phys. Rev. 128, 2131 (1962).

[52]R. J. Birgeneau, R. Dingle, M. T. Hutchings, G. Shirane, and S. L. Holt, Phys. Rev. Letters 26, 718 (1971); M. Blume, R. E. Watson, and G. H. Vineyard, Bull. Am. Phys. Soc. 16, 629 (1971).

[53]J. C. Bonner and M. E. Fisher, Phys Rev. 135, A640 (1964).

[54]Previous attempts to apply the one-dimensional Hubbard model to molecular systems and/or molecular crystals include the work of Ovchinnikov (Ref. 16) and Musurkin and Ovchinnikov (Ref. 17), as well as the following: P. J. Strebel and Z. G. Soos, J. Chem. Phys. 53, 4077 (1970); D. J. Klein and Z. G. Soos, Mol. Phys. 20, 1013 (1971).

[55]C. G. Kuper, Phys. Rev. 150, 189 (1966).

[56]D. R. Penn, Phys. Rev. 128, 2093 (1962).

[57]L. I. Buravov, M. L. Khidekel', I. F. Shchegolev, and E. B. Yagubskii, Zh. Eksperim. i Teor. Fiz. Pis'ma v Redaktsiyu 12, 142 (1970) [Sov. Phys. JETP Letters 12, 99 (1970)].

[58]L. Falicov and R. Harris, J. Chem. Phys. 51, 3153 (1969).

[59]M. Takahashi, Progr. Theoret. Phys. (Kyoto) 45, 756 (1971).

[60]G. Rickayzen, *Theory of Superconductivity* (Interscience, New York, 1965).

[61]R. B. Griffiths, Phys. Rev. 133, A768 (1964).

[62]J. I. Katz, S. A. Rice, S. Choi, and J. Jortner, J. Chem. Phys. 39, 1683 (1963).

[63]P. Devaux and G. Delacote, Chem. Phys. Letters 2, 237 (1968).

[64]M. Sukigara and R. C. Nelson, Mol. Phys. 17, 387 (1969).

[65]J. Kanamori, Progr. Theoret. Phys. (Kyoto) 30, 275 (1963); see also R. Dapree and D. J. W. Geldart, Solid State Commun. 9, 145 (1971).

[66]W. E. Evenson, J. R. Schrieffer, and S. Q. Wang, J. Appl. Phys. 41, 1199 (1970).

[67]N. F. Mott, J. Phys. (Paris) 32, C1-11 (1971).

[68]L. D. Landau, Zh. Eksperim. i Teor. Fiz. 30, 1058 (1956) [Sov. Phys. JETP 3, 920 (1957)]; and other papers reprinted in D. Pines, *The Many-Body Problem* (Benjamin, New York, 1962).

[69]J. M. Ziman, *Electrons and Phonons* (Oxford U. P., London, 1960).

[70]H. M. Rosenberg, *Low Temperature Solid State Physics* (Clarendon, London, 1963).

[71]Preliminary measurements of the thermal conductivity on compacted powder samples indicate an increase with increasing temperature up to about 200 °K. Above 200 °K, the thermal conductivity is temperature independent, characteristic of a metal.

[72]Kinshiro Hirakawa, Kazuyoshi Hirakawa, and Takasu Hashimoto, J. Phys. Soc. Japan 15, 2063 (1960); S. Kadota, I. Yamada, S. Yoneyama, and K. Hirakawa, *ibid.* 23, 751 (1967); K. Hirakawa and S. Kadota, *ibid.* 23, 756 (1967); M. T. Hutchings, E. J. Samuelson, G. Shirane, and K. Hiradawa, Phys. Rev. 188, 919 (1969); for analysis of $CuCl_2 \cdot 2NC_5H_5$, see K. Takeda, S. Matsukawa, and T. Haseda, J. Phys. Soc. Japan 30,

1330 (1970).
[73]T. Nagamiya, Progr. Theoret. Phys. (Kyoto) 6, 342 (1951); C. Kittel, Phys. Rev. 82, 565 (1951); F. Keffer and C. Kittel, *ibid.* 85, 329 (1952).
[74]P. W. Anderson, Phys. Rev. 86, 694 (1952).
[75]P. W. Anderson and P. R. Weiss, Rev. Mod. Phys. 25, 269 (1953).
[76]R. Kubo and K. Tomita, J. Phys. Soc. Japan 9, 888 (1954).
[77]J. H. Van Vleck, Phys. Rev. 74, 1168 (1948).
[78]A. Münster, in *Fluctuation Phenomena in Solids*, edited by R. E. Burgess (Academic, New York, 1965).
[79]L. R. Maxwell and T. R. McGuire, Rev. Mod. Phys. 25, 279 (1953).
[80]C. N. Yang, Rev. Mod. Phys. 34, 694 (1962); R. A. Ferrell, Phys. Rev. Letters 13, 330 (1964); T. M. Rice, Phys. Rev. 140, A1889 (1965).
[81]F. Carboni and P. M. Richards, Phys. Rev. 177, 889 (1969).
[82]R. E. Dietz, F. R. Merritt, R. Dingle, D. Hone, B. G. Silbernagel, and P. M. Richards, Phys. Rev. Letters 26, 1186 (1971).
[83]A. W. Overhauser, Phys. Rev. 89, 689 (1953).
[84]R. J. Elliott, Phys. Rev. 96, 266 (1954).
[85]Y. Yafet, in *Solid State Physics*, edited by F. Seitz and D. Turnbull (Academic, New York, 1963), Vol. 14.
[86]J. M. Ziman, *Principles of the Theory of Solids* (Cambridge U. P., London, 1964), p. 182.
[87]A. J. Epstein, thesis (University of Pennsylvania, 1971) (unpublished).
[88]Y. Iida, Bull. Chem. Soc. Japan 42, 71 (1969).
[89]*Proceedings of the International Conference on Organic Superconductors*, edited by W. A. Little (Interscience, New York, 1970); V. L. Ginzburg, Contemp. Phys. 9, 355 (1968).
[90]J. R. Schrieffer, *Theory of Superconductivity* (Benjamin, New York, 1964).
[91]One must be somewhat careful here, for if U_0 is made too small, a charge-density wave insulator is likely to result, see R. A. Bari, Phys. Rev. B 3, 2662 (1971).
[92]J. M. Zimaun, *Electrons and Phonons* (Oxford U. P., London, 1960), p. 212.
[93]D. P. Craig and S. H. Walmsley, in *Physics of Chemistry of the Organic Solid State*, edited by M. M. Labes and D. Fox (Interscience, New York, 1967), Vol. 1; S. A. Rice and J. Jortiner, *ibid.*, Vol. 3.
[94]P. W. Anderson, Phys. Rev. 109, 1432 (1958).

PHYSICAL REVIEW B VOLUME 5, NUMBER 3 1 FEBRUARY 1972

Thermodynamics of the Heisenberg Ferromagnet in an Applied Magnetic Field

Lawrence Flax
Lewis Research Center, National Aeronautics and Space Administration, Cleveland, Ohio 44135
(Received 2 June 1971)

The anisotropic-Heisenberg-ferromagnet formalism developed previously is examined to include an applied magnetic field for the isotropic case in the random-phase approximation. Thermodynamic quantities such as magnetization, susceptibility, and the derivative of magnetization with respect to temperature are studied near the Curie point.

INTRODUCTION

According to the Weiss theory, a ferromagnetic material possesses an internal field which is proportional to the magnetization. As the temperature of a ferromagnet is increased, the magnetization decreases until, at a temperature known as the Curie temperature T_c, the material becomes paramagnetic. This change from ferromagnetism to paramagnetism is referred to as the ferromagnetic-phase transition. Experiments and theory have shown that electrical, mechanical, and many thermodynamic properties of a material are altered when the material undergoes a phase transition.

The effect of an external magnetic field is twofold: (i) The magnetization is increased above its zero-field value and (ii) the transition region is broadened. Even though increasing temperature tends to destroy spin alignment, the field causes some ordering to be present. Thus, instead of an abrupt change at the critical temperature there is a more gradual transition.

This report investigates some thermodynamic properties of the Heisenberg ferromagnet in an external magnetic field. The quantities studied are the magnetization, susceptibility, and the derivative of magnetization with respect to temperature. The last of these can be used to calculate entropy and the magnetocaloric effect, which are useful for investigating various recently proposed magnetic refrigeration systems.[1,2]

Model

The Heisenberg model assumes the magnetic electrons are in states localized about the lattice sites with an exchange interaction taking place between electrons. The model does not take into account itinerant electrons and is considered valid for insulating ferromagnets such as EuO but not for conductors such as iron and nickel. However, it appears that this model gives better results for conductors at low temperatures than those calculat-